R. & M. No. 3797

R. & M. No. 3797

PROCUREMENT EXECUTIVE MINISTRY OF DEFENCE

AERONAUTICAL RESEARCH COUNCIL

REPORTS AND MEMORANDA

Experience with a Steady-State Heat-Transfer Technique in a Large Wind-Tunnel

By K. G. WINTER, L. GAUDET AND T. G. GELL

Aerodynamics Dept., R.A.E., Bedford

LONDON: HER MAJESTY'S STATIONERY OFFICE

1977

£5 net

Experience with a Steady-State Heat-Transfer Technique in a Large Wind-Tunnel

By K. G. WINTER, L. GAUDET AND T. G. GELL

Aerodynamics Dept., R.A.E., Bedford

Reports and Memoranda No. 3797*
April, 1975

Summary

The Report covers the design and development of a plant for pumping a liquid through a model so as to control its temperature, the design and manufacture of the model, and the development of the heat-flow meters used in the model and the means of calibrating them.

Sample measurements of heat transfer on the model, a rhombic cone of unit aspect ratio at a Mach number of 2·45, are shown and compared with calculated values.

* Replaces R.A.E. Technical Report 75020—A.R.C. 36 202

LIST OF CONTENTS

1. Introduction

In short-duration wind tunnels, the measurement of aerodynamic heat transfer distributions on models is relatively straightforward[1] using instrumented thin-skinned models, or even non-instrumented models with temperature-sensitive surface coatings. The same techniques can be carried over to continuous wind tunnels, providing arrangements can be made, either for rapid insertion of the model into the airstream[2], or for shields, enclosing the model[3], which can be retracted rapidly. (Such shields may also be required in intermittent tunnels to avoid problems with starting transients.) The temperature of the model is adjusted to a required value whilst it is withdrawn from the airstream or enclosed by the shields. In the design of heat-transfer systems for the R.A.E. 8 ft × 8 ft and 3 ft × 4 ft wind tunnels the use of the transient technique was considered but it was decided that the special engineering required would be too extensive, particularly for the 8 ft × 8 ft tunnel (shown in Fig. 1), and would have involved too much loss of operating time both in the initial modifications required to the tunnels, and in subsequent installation for heat transfer tests. Instead, it was decided to adopt a steady-state technique and to arrange for controlled variation of model temperature as described in the next section.

2. Cooling-Plant Design

Several factors influenced the requirements for the cooling plant, the main ones being:

(i) the estimated maximum heat transfer to the largest models which could be tested,
(ii) the accuracy with which temperatures and heat flow might be measured,
(iii) practical limitations in maintaining low temperatures,
(iv) the degradation of material properties at low temperatures.

On the basis of these factors the broad specification of the cooling plant was that it should be capable of maintaining a model surface temperature of $-60°C$ whilst extracting heat at a rate of 40 kW. It was also specified that, for the maximum rate of heat extraction, the temperature rise of the coolant in passing through the model should not exceed 5°C in order that large temperature gradients in the model should not occur. Furthermore, to make the process of determining model surface recovery temperatures one of interpolation rather than extrapolation it was considered desirable that the cooling system should also be capable of adding heat to the model.

The basic choice to be made in the cooling plant was the cooling medium. Possibilities considered were liquids having low freezing points, or liquified gases such as liquid nitrogen. The latter were discarded because of the difficulties of control and also because of the virtual impossibility of also heating a model with the same medium as that used for cooling. There had been previous experience[4] within R.A.E. in small wind tunnels in the use of a steady-state technique in which the model was cooled by alcohol pumped through it, the alcohol being cooled by passing it through a vessel containing a mixture of alcohol and solid carbon dioxide. In principle the same system was adopted, but possible fire hazards in the large facilities precluded the use of alcohol. Instead trichlorethylene was adopted in blithe ignorance of the dangers involved. Two of these dangers are the spontaneous decomposition of trichlorethylene to produce hydrochloric acid vapour and the disintegration of the plastics, commonly used in insulating wiring, in the presence of trichlorethylene vapour. Recent developments in inhibitors in trichlorethylene have reduced the chances of the first of these occurring.

An outline of the circuit is shown in Fig. 2. The specification implied that the maximum flow of the coolant should be about $4\frac{1}{2}$ litres (1 gallon) per second. At the maximum heat extraction rate the consumption of solid carbon dioxide was estimated to be about 200 kg per hour and hence it was necessary to provide mechanical means for crushing the blocks and feeding the resultant material to the mixing tank. It was envisaged that model temperature would be controlled by setting the manually-operated valves governing the rate of flow of the coolant in the secondary circuit through the heat-exchanger, and at the same time controlling the flow into the model by operation of the motorised valves, MV_1 and MV_3 from the tunnel observation room, with MV_2 being left fully open. In the event, as shown later, more precise control was obtained by cooling the secondary fluid to a lower temperature than required and using the heater in a servo-loop linked to the coolant temperature as indicated in Fig. 2.

One problem of design was to maintain adequate size of pipes in the secondary circuit to avoid unduly large pressure drops, and consequent heat production. Where the supply passed through the model support mechanism and sting, long lengths (4 m) of small-bore pipe (27 mm) were inevitable and the associated large pressure drop unavoidable. The total pressure loss in the secondary circuit at full mass flow is 600 kPa requiring a pump of 8 kW power. It was envisaged initially that PTFE pipes would be required to meet strength and flexibility requirements for the supply through the model support. However, the material available

(paste-extruded PTFE) proved to be brittle and the final arrangement uses nylon pipes, which have been found to have enough flexibility to enable the model to be rolled through $\pm 180°$, with the necessity of providing special joints only for the 3 ft × 4 ft tunnel in which the length available for twisting is appreciably shorter than for the 8 ft × 8 ft tunnel. The flexibility to meet variation of the angle of incidence of the model is provided by larger (75 mm bore) metal flexible hoses lined with PTFE.

3. Model Design

3.1. General Remarks

Two aspects of model design need careful consideration. The first is the arrangement of the internal cooling system so that sufficient heat can be extracted from the model to match the aerodynamic heat transfer at low values of wall temperature, and the second is to choose the thermal conductivity of the skin so that sufficiently large values of temperature difference across it may be obtained to give a sensitive measure of heat transfer, whilst still maintaining the capability of obtaining low values of wall temperature.

The model discussed in this Report uses a series of small-bore pipes connected in parallel to inlet and outlet manifolds. The design was based on the simple ideas outlined below.

The relation between Nusselt, Reynolds and Prandtl numbers for the flow through a circular pipe is given by the empirical formula (see, for example, McAdams[5])

$$\mathrm{Nu} = 0{\cdot}23\,\mathrm{Re}^{0{\cdot}8}\,\mathrm{Pr}^{0{\cdot}4}, \qquad \mathrm{Re} > 2100 \tag{1}$$

where

$$\mathrm{Nu} = \frac{hd}{k\Delta T}, \qquad \mathrm{Re} = \frac{\rho \bar{u} d}{\mu}, \qquad \mathrm{Pr} = \frac{\mu C_p}{k}$$

with

h rate of heat flow per unit area
d diameter of pipe
k thermal conductivity of coolant
ρ density of coolant
$\bar{u}$ mean velocity through pipe
μ viscosity of coolant
C_p specific heat of coolant
ΔT temperature difference between pipe and cooolant.

Suppose that a model has a mean span s and that the internal surfaces are completely covered by a series of parallel tubes each of which is of length twice that of the model. These are connected together through manifolds so that each tube carries the same flow of coolant. The model will then be covered by N tubes of diameter d where $Nd = s$. If the total mass flow of coolant through the model is m, and if the thickness of the walls of tubes is neglected, then,

$$\mathrm{Re} = \frac{\rho \bar{u} d}{\mu} = \frac{md}{(\pi/4)d^2 N\mu} \propto \frac{m}{Nd} = \frac{m}{s} = \text{const.} \tag{2}$$

Therefore Nu = constant, independent of the number of tubes, for a given substance as the coolant and the rate of heat flow, h, is given by

$$h = \frac{k\mathrm{Nu}\Delta T}{d} \propto \frac{1}{d} \tag{3}$$

for given temperatures.

Hence, for a given coolant supply, the heat transfer capability increases in inverse proportion to d, and so the smallest pipes compatible with an acceptable pressure drop should be used.

In the model design considered, the heat flow is derived by measuring the temperature gradient through a resin skin (which may be loaded with a suitable filler to vary its properties). The complete heat path from the air flowing over the model to the coolant then passes through four regions,

(1) airflow to model surface
(2) the model skin
(3) a metal structural shell and the walls of the cooling tubes
(4) a convective path between the inner walls of the tubes and the coolant.

If the model skin were made of a material of high thermal conductivity then low wall-temperatures and high aerodynamic heat transfer rates could be obtained, but the temperature difference across the skin would be small and the accuracy to which the heat transfer could be measured would consequently also be small. Intuitively one therefore expects that a choice for the model skin can be made, which will be an optimum with respect to the sensitivity of the system. An attempt can be made to obtain a formal maximum for the sensitivity in the following way. At equilibrium conditions the heat flow through each of the regions, taken as being one-dimensional, is the same. Thus,

$$h = a_a(T_r - T_w) \tag{4}$$

$$h = a_s(T_w - T_b) \tag{5}$$

$$h = a_c(T_b - T_c) \tag{6}$$

where

h is the heat flow per unit area per unit time
a_a is an aerodynamic heat-transfer coefficient
a_s is a measure of the skin conductivity $(= k/l)$

and regions (3) and (4) have been lumped together to give a combined conductivity, a_c, for the metal shell, the tube walls and convective heat transfer to the coolant; T_r, T_w, T_b and T_c are respectively the aerodynamic recovery temperature, the wall temperature, the temperature at the inner surface of the skin and the coolant temperature.

A criterion of the sensitivity of the measuring system is

$$\frac{\partial}{\partial a_a}(T_w - T_b),$$

which is effectively the rate of change of the signal measured, with the aerodynamic heat-transfer coefficient*. From equations (4), (5) and (6)

$$T_w - T_b = \left(\frac{T_r - T_c}{a_s}\right)\frac{1}{(1/a_a)+(1/a_s)+(1/a_c)}$$

and hence the sensitivity,

$$S = \frac{\partial(T_w - T_b)}{\partial a_a} = \frac{T_r - T_c}{a_s a_a^2}\,\frac{1}{[(1/a_a)+(1/a_s)+(1/a_c)]^2}. \tag{7}$$

A formal maximum can be obtained by specifying

$$\frac{\partial S}{\partial a_s} = 0$$

i.e.

$$\frac{T_r - T_c}{[(1/a_a)+(1/a_s)+(1/a_c)]^3 a_s^3 a_a^2}\left(1 - \frac{a_s}{a_a} - \frac{a_s}{a_c}\right) = 0. \tag{8}$$

* It is assumed that the electrical signal from a heat-flow meter will vary linearly with the temperature difference to which it is subjected.

Therefore for maximum sensitivity

$$\frac{1}{a_s}=\frac{1}{a_a}+\frac{1}{a_c} \tag{9}$$

by which is implied from equations (4), (5) and (6) that

$$2(T_w-T_b)=T_r-T_c. \tag{10}$$

Equation (10) thus indicates that for optimum sensitivity the temperature drop through the skin should be half the total drop in temperature from the air recovery temperature to the coolant temperature. This result obviously cannot be met for a range of conditions, in which the aerodynamic heat-transfer coefficients vary, and its strict application would lead to undesirably high values of wall temperature. Another consideration in choosing the thermal conductivity of the skin is the time to respond to changes of temperature. This would probably be too long with the 'optimum-sensitivity' skin. For the rhombic cone model discussed subsequently the conductivity of the skin was chosen to be higher than that given by equation (9).

3.2. Rhombic-Cone Model

The model tested is a rhombic cone of unit planform aspect ratio, and with leading-edge angle (normal to the centre-line) of 30 degrees. It was chosen for a number of reasons. Structurally, it was simple to design and could be carried easily on the tunnel model-support mechanism. Aerodynamically, at zero angle of incidence, the boundary-layer development would be close to that on a flat plate so that comparison could be made with previous data, and at other angles of incidence a complex three-dimensional flow would be obtained; the information would also be of direct relevance to slender-wing aircraft.

A sketch of the model is shown in Fig. 3. On the basis of the considerations in the previous section coolant tubes of 6 mm bore were chosen to be attached to a steel shell 2.5 mm thick. This shell was made in two halves attached together along the leading edges and supported via insulating bushes from a mounting tongue which terminated externally in the standard taper joint of the model-support system. The layout of the coolant tubes resulted from a fairly extensive drafting exercise. It was clear, because of the shape of the model, that it would be difficult to cover all the internal surfaces with tubes of equal length in parallel; instead the aim was to cover as uniformly as possible the port half of the upper surface and the starboard half of the lower surface. The main arrays of heat-flow meters were installed on one surface and pressure-plotting points on the other. The cooling tubes were fitted in three banks along the length of the model. The nose section was treated differently and was made from a copper block through which were drilled passages for the coolant. The pressure drop of the coolant in flowing through the tubes was not well matched between tubes because of differing lengths and of different numbers of bends, and because of non-uniformities in the flow in the manifolds. To improve the matching, flow-control valves were fitted in the outlet manifolds and adjusted before final assembly of the model. Unfortunately the extra restriction reduced considerably the coolant flow from a possible maximum of $4\frac{1}{2}$ litres per second to about $1\frac{1}{2}$ litres per second. Because of difficulties of supply of stainless steel tubing mild steel was used. This was a mistake because it has proved almost impossible to avoid corrosion, the cleansing action of the trichlorethylene making immediate rapid corrosion occur if surfaces are subsequently exposed to the atmosphere.

The tubes are attached to the skin by soldering. To ensure that no voids in the solder occurred, which would have distorted the heat-flow paths, completed sections of the assemblies were X-rayed at appropriate stages. Examples of good and bad soldering are shown as the upper and lower photographs in Fig. 4.

The skin material was chosen to have the same thermal conductivity as the tellurium-silver heat-flow meters[4,6] which it was initially intended to use, but which were abandoned subsequently, as discussed later. Thus the only way in which the overall conductivity of the skin could be varied to meet the compromise requirements outlined previously was by variation of the skin thickness. This was chosen to be 1·52 mm. The choice of the material for the skin followed that of Naysmith[4] who used a resin loaded with aluminium powder to achieve the required thermal conductivity. However, although Naysmith did not have difficulty with his small flat-plate model, it was found that on large test pieces, or on shapes with external corners, cracking of the skin occurred on cooling to low temperatures, leading to loss of adhesion to a steel shell. In view of Naysmith's experience and of the properties of the material (the coefficient of thermal expansion and tensile strength at low temperatures), this problem was unexpected. It was assumed that the properties of the material cast on a steel shell were inferior to those of an isolated casting but a proper explanation was not found. However, the problem was resolved when it was discovered that, if the steel shell were first coated with a layer of resin rubber which was also loaded with aluminium powder to modify its thermal conductivity, the skin would survive the expected temperature changes. The final model skin was therefore cast in two layers; the lower layer had a

thickness of one third that of the total and was of resin rubber, and the upper was of the harder resin. The details of the preparation of the skin material are given in the Appendix.

Seventy-one heat-flow meters (of bead thermocouple type) and fifty-three pressure tappings were built into the skin during the casting process. The main arrays of meters were installed on the port upper surface in three spanwise rows and also in two further rows, one at 70 per cent semi-span and one close to the ridge line as shown in Fig. 5. A few meters were also fitted in the starboard upper surface. Two heat-flow meters were positioned in the lower starboard surface to give a check on the symmetry of the heat flow through the two surfaces. The meters were inset into the sub-layer of resin rubber, and their electrical leads were taken to the model trailing edge, before the outer resin skin was cast. At the trailing edge of the model where the thermocouple wires emerge, the protruding wires were encased in a casting of cold-setting rubber to reduce the possibility of breakages and short circuits occurring.

The static pressure holes in the model surface were fitted in diametrically opposite faces of the model to the heat-flow meters. The pressure tubes were led through the steel shell at the measuring points and soldered into position. A hollow cap was fitted over each tube before casting the resin skin and the surface pressure holes were drilled through the resin into the cap.

A photograph of the finished model mounted in the 8 ft × 8 ft tunnel is shown in Fig. 6.

4. Heat-Flow Meters

4.1. General Requirements

There are several factors to be taken into account in the design of a steady-state heat-flow meter for aerodynamic testing:

(a) Heat flow through the surface of interest should not be significantly disturbed by the presence of the meter, that is the thermal conductivity and the emissivity of the meter should match its surroundings.

(b) There must be no disturbance to the airflow over the surface.

(c) The meter should measure both the rate of heat flow through the surface and the surface temperature at the same point.

(d) The meter should be as small as possible in order that detailed spatial variations in heat flow may be measured.

(e) An adequate electrical signal should be produced. For the test conditions considered specifically in this Report the maximum heat flow was estimated to be about 30 kW m^{-2} and the aim was to measure to an accuracy of 0·1 per cent of this value. The recording system to be used was capable of resolving to 1 μV so that it was desirable that the sensitivity of a meter should be such as to generate at least 1 μV for a heat flow of 30 W m^{-2}.

4.2. Specific Designs

Many different heat-flow meters have been designed and used in the past; none of them was considered completely satisfactory for the present application. Most of the devices are based on obtaining heat flow by the measurement of temperature difference across a skin of known thermal conductivity, and differ only in the type of transducer used to relate the temperature to an electrical signal. Some of the exceptions use a deliberate distortion of the heat-flow field in order to create temperature gradients in a more convenient direction.

A brief review of some of the available instruments is given below. Included are some developments which took place subsequent to the investigations described in Section 4.3.

Circular foil (Plenier[7], Gardon[8], Northover and Hitchcock[9])

A foil of constantan is carried on the end of a cylindrical copper sleeve and a copper wire is attached to the centre of the foil. The copper sleeve fits in a hole through the wall and the constantan foil is flush with the surface.

The heat flow into or out of the foil is conducted through the foil to the copper sleeve and the thermal resistance of the foil creates a radial temperature gradient which is measured by the voltage between the copper wire and the copper sleeve. Other thermoelectric pairs of materials could be used.

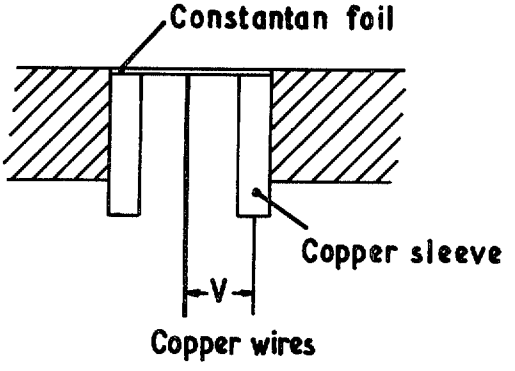

The heat flow is given by

$$h = \frac{4kl}{R^2}\Delta T$$

where

R is the radius of the disc,
l its thickness and k its thermal conductivity.

For a small meter, 1 mm diameter with a constantan foil 0·02 mm thick this gives a sensitivity of roughly 50 μV kW^{-1} m^2.

Trimmer *et al.*[10] describes a version of the foil gauge in which the sensitivity is enhanced by using deposited films of antimony and bismuth to form a thermopile arrangement.

The disadvantages of the meter are the need to provide a separate means of measuring surface temperature and the distortion in surface temperature created by both the foil and the copper sink.

Thin-foil differential thermocouple (Hager[11])

Edge-welded copper–constantan thermocouple ribbon is folded over a film of a suitable insulating material and the ribbon is cut so as to form a differential thermocouple.

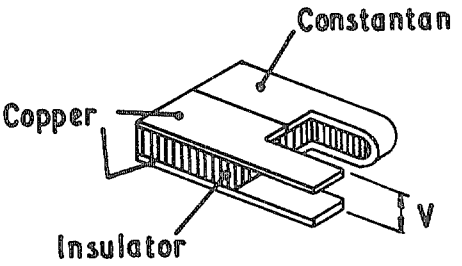

Hager made meters of various values of thickness, the smallest having a foil thickness of 0·006 mm and an insulation layer 0·125 mm thick. The heat flow is given approximately by

$$h = \frac{k}{l}\Delta T$$

where l is the thickness of the insulation layer and k its thermal conductivity.

For a meter of total thickness 0·137 mm and a plastics interlayer of thermal conductivity 0·2 W m^{-1} K^{-1} the sensitivity is about 30 μV kW^{-1} m^2.

The meter could have been installed in the present model with the insulation material and thickness chosen to meet the particular requirements. Its use in such a model would necessitate a means of providing a separate measurement of surface temperature.

Tellurium-silver block (Hatfield and Wilkins[6])

Hatfield and Wilkins, noting the high figure of merit* of a combination of tellurium–silver and copper made heat meters of a disc of tellurium–silver with copper-gauze discs bonded on each side to produce a differential thermocouple. The discs were 12·7 mm diameter and 1·27 mm thick. The sensitivity derived from the properties of the material is about 500 μV kW^{-1} m^2. Naysmith used meters of this type which he embedded in a resin skin which was loaded with aluminium powder so that its thermal conductivity matched that of the meters. Separate thermocouples had to be provided to measure surface temperature. Attempts to develop a miniature version of this type of meter are described in Section 4.3.

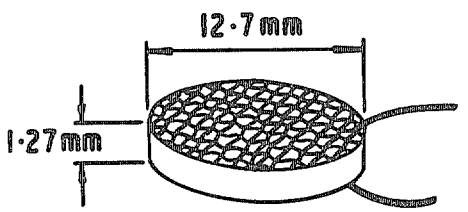

Schulte and Kohl[12] investigated the use of silver–antimony–telluride over a large temperature range, 80 K to 320 K, and noted that its figure of merit varied by a factor of about 2:1 over this range. They devised a means of compensating for this variation in a heat-flow meter, in which it was arranged to have parallel heat paths through silver–antimony–telluride and an epoxy resin, with the cross-sectional area of the two materials

* The figure of merit is defined as the ratio of the thermoelectric coefficient of a pair of materials to the thermal conductivity of one of them. The value for tellurium–silver : copper is about 400 μV W^{-1} m compared with 0·1 μV W^{-1} m for copper : constantan.

so chosen that the variation in thermal conductivity of the resin compensated for the changes in both the thermal conductivity and thermo-electric coefficient of the silver–antimony–telluride. The meter was constructed by making orthogonal sawcuts, which were filled with resin, through a thin sheet of silver–antimony–telluride, so that an array of square prisms embedded in resin was produced. The prisms were made into a thermopile by connections of silver paint taken through the resin in small drilled holes. Copper foil was bonded on both sides of the meter by epoxy cement, with the purpose of making each side of the meter isothermal. For a meter 1·4 mm thick containing 45 elements they obtained the large sensitivity of 25 mV kW^{-1} m^2.

Schulte and Kohl[13] also investigated the use of a combination of 'n' and 'p' doped germanium for which they quote a thermo-electric coefficient of 1·8 Mv/K.

Twin thermocouple

The twin-thermocouple meter used in the present investigation is described in Section 4.3. A rather elaborate form of a twin-thermocouple meter is described by Laumann[14]. The heat path is provided by a cylinder of Teflon of 3·8 mm diameter and 5·1 mm length, one face of which forms part of the airswept surface and the other face butts against an aluminium block. The curved surface of the cylinder is surrounded by an insulation material called Tipersul which in turn is surrounded by a metal sleeve into which the aluminium block fits. When the meter is installed in a model the metal surfaces are internal to the model and are cooled. The temperatures at the ends of the Teflon cylinder are measured by chromel–constantan thermocouples, the leads from which emerge through the aluminium block. The leads to the thermocouple in the exposed face are spirally wound round the cylinder to reduce heat conduction effects.

The results from this meter must be uncertain because of the large distortions to the surface temperature which it may be expected to create.

Thermopile (Hartwig *et al.*[15,16], Hornbaker and Rall[17])

The sensitivity of a differential thermocouple pair is increased by arranging to have a number of pairs of thermocouples in series. Hartwig *et al.* effected a neat solution to the problem of manufacture by winding a constantan wire round a glass slide and then silver plating one half so that a series of silver–constantan thermojunctions was formed. Their meter had fifty turns of 0·025 mm diameter wire on a glass slide $3{\cdot}2 \times 1{\cdot}6 \times 0{\cdot}18$ mm, and gave a sensitivity of about 260 μV kW^{-1} m^2. In application the meter was embedded in a skin of porcelain.

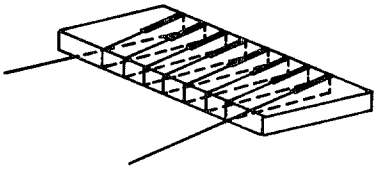

A separate means of measuring surface temperature is not provided by this meter and there must be some doubt in the results obtained from it because of the heat paths provided by the windings.

Thin-film resistors (Johnson[18])

Johnson made a meter in which the temperature-measuring elements were platinum films fired onto both sides of a ceramic disc of about 10 mm diameter. Platinum leads were connected by silver paint to extensions to the films, the resistance of which was reduced by gold overlays. With the energizing current to the films kept sufficiently small to make self-heating effects of the films negligible a sensitivity of about 150 μV kW^{-1} m^2 was obtained.

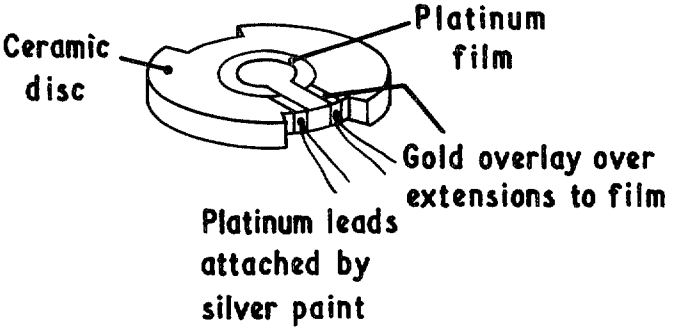

One disadvantage of resistive elements is that they are passive, that is to say they require both supply and signal leads. In common with thin-film thermocouples they can be deposited reliably only on particular substrates.

Thermistors[19] might also be used as temperature-sensing elements and would probably enable very small temperature gradients to be measured but, presumably because of their bulk, they appear not to have been applied to heat-flow meters.

For the future, thin-film devices[20] seem to be the most promising but they had not reached a sufficiently practical stage of development at the time of the work described in this Report.

4.3. Types of Heat-Flow Meter Evaluated

4.3.1. General

Four types of heat-flow meter were evaluated, all of which used active thermoelectric devices. These were:

(i) semiconductor (tellurium–silver)
(ii) thin bismuth film
(iii) differential bead thermocouples
(iv) separate bead thermocouples.

In addition some work was done on thin-film thermocouples but the problems of satisfactory deposition on a resin substrate, and of bonding the films to lead wires were not overcome in time.

4.3.2. Semiconductor Meters

The meters (Hatfield & Wilkins[6]) described in Section 4.2 were considered to be too large for the present application and are not provided with a means of measuring surface temperature. A development contract was therefore placed with industry in 1961 for a smaller device. This was to contain a cube of tellurium–silver of length of side 1·25 mm, and was to be provided with a surface thermocouple. The essential problem in obtaining reproducible performance from these small meters was found to be in the bonding of the leads. The fine copper mesh used on the Hatfield meters was unsatisfactory for the smaller areas involved. Apparent success was obtained with the thermocompression bonding of gold leads. However, calibrations for five nominally identical tellurium–silver heat-flow meters of the type shown in Fig. 7a differed in sensitivity by a factor of 3, and it was decided that a reliable device could not be produced using the thermocompression processs. Furthermore, calibrations made in R.A.E. using a form of Lees disc calibrator gave values for the sensitivity of large-size tellurium–silver meters of about 60 per cent of that obtained by Hatfield or quoted for commercially-available meters. Suspicion was cast on the Hatfield[6] type of calibrator (Fig. 8) as discussed later (Section 5.2).

It became clear at this stage that it was unlikely that a reliable semiconductor meter of small size, which also incorporated a means of measuring surface temperature, could be developed in time to be used in the model, described earlier, which was being manufactured. Accordingly attention was turned to providing simple meters using two copper–constantan bead thermocouples, the considerable reduction in sensitivity which this entailed being accepted. The performance of these meters, which were used in the model, is described subsequently. Meanwhile limited investigations of other types of meters continued.

4.3.3. Thin Bismuth-Film Meter

One of the disadvantages of using a solid block of semi-conductor material, as in the tellurium–silver meters, is that the surrounding material, the skin of a model, should have a thermal conductivity the same as the semi-conductor to avoid distortion of the heat flow through the meter. This disadvantage could be avoided if the volume of the semi-conductor material could be made very small, whilst a finite length of material existed in the direction of the heat flow. In other words a thin film of material with the plane of the film normal to the surface of the meter would have negligible thermal inertia and would take up the temperature of the surrounding material. Suitable connections at its ends would provide a differential thermocouple. Experience at the time suggested that, of possible materials, bismuth could most readily be deposited as a thin film on a resin surface. Two experimental meters were made and tested. The bismuth was deposited across the gap between two copper wires set in the aluminium-resin mixture, completing a connection between the wires and forming a differential thermocouple. The meters were then completed by casting further resin over the film. The film was of length 1·5 mm set in a disc 2·5 mm thick, of diameter 35·5 mm. On the basis of the properties of the disc material and the thermoelectric properties of bismuth–copper junctions a sensitivity of about 120 μV kW^{-1} m^2 would have been expected. In fact the sensitivity measured in the prototype version of the modified Lees disc type calibrator (Section 5.4) was about 80 μV kW^{-1} m^2.

Some difficulties were encountered when a meter was reversed in the calibrator. It was noticed that the resistances, which were intially 63 ohms and 85 ohms for the two devices, varied quite markedly. The likely cause of this variation was unsatisfactory bonding of the bismuth to the copper wires. Investigation of alternative manufacturing techniques to improve the bonding was not pursued but the idea probably merits further study.

4.3.4. Bead Thermocouple Meters

Because of the failure to develop reliable heat-flow meters of sophisticated design, attention was turned to simpler devices which used bead thermocouples. An attempt was made to produce a meter which would have its two output signals primarily related individually to the heat flow and the surface temperature. This design incorporated four thermocouples, three of which were in line on the windswept surface. The centre one of these was connected differentially to the one on the opposite face to measure heat flow, and the other two were connected in parallel to give an average temperature, which it was expected would be close to the surface temperature at the centre thermocouple. Tests showed that this type of device was unreliable because of the number of interconnections and probably it would have been inaccurate also because of the extraneous heat paths provided by the wires. Ultimately the simplest type of device was adopted which had one bead thermocouple on each face.

The arrangement of such a meter is shown schematically in Fig. 7b and a photograph is shown in Fig. 9. The meter consists of a flat block of epoxy resin loaded with aluminium powder (see the Appendix), in which two fine-wire copper–constantan thermocouples are embedded. The composition of the block is chosen so that its thermal conductivity matches that of the model skin. To reduce the effects on the heat flow, of the high thermal conductivity of the copper and constantan wire used for the thermocouples, the wires are of very small diameter (0·1 mm) for a length of 10 mm from the bead and are then joined to 0·275 mm diameter wire to produce robust external connections (Fig. 10). The maximum temperature difference, across a meter of thermal conductivity 1·05 $W\,m^{-1}\,°C^{-1}$ and thickness 1·52 mm for a heat flow of 30 $kW\,m^{-2}$, is 45 °C. Thus for thermocouple sensitivities of 40 $\mu V\,°C^{-1}$ the output voltage is 1·8 mV, and the meter should meet the requirement given in Section 4.1.

A future development for thermocouple-type meters would be in the use of deposited thin-film thermocouples such as shown in Fig. 7c.

5. Calibration Techniques

5.1. Introduction

In order to evaluate the characteristics of heat-flow meters of different types a calibration device was needed. Of the three fundamental methods of providing heat flow for steady-state calibration, namely by convection, conduction or radiation[21], it was considered that a conductive type calibrator would offer the most practicable solution.

The Hatfield calibrator, as mentioned earlier, was not considered to be suitable and so a series of R.A.E. calibrators evolved. These and the Hatfield calibrator are described below.

5.2. Hatfield Calibrator

This device (Fig. 8) described by Hatfield and Wilkins[6] consisted of layers of thick furniture plush lying on top of a plate heater. This stack was surrounded by a similar arrangement to form a guard for the sides and to prevent heat escaping laterally. A second guard heater was placed underneath the main heater to prevent heat escaping downwards. On top of the furniture plush was placed a copper sheet from which heat naturally convected to the atmosphere.

The calibration technique was to insert heat-flow meters between the layers of plush and to supply the main heater with a constant power. A stabilising period of several hours was then necessary during which the guard heaters were trimmed until pairs of monitoring thermocouples, situated on the guards and main heater, indicated minimum heat loss.

This method of calibration was not thought to be suitable for R.A.E. requirements for four main reasons:

(1) It was considered that the insertion of heatmeters of thermal conductivity some 20 times that of the plush would cause a distortion in the heat flow path and would result in an erroneously high apparent sensitivity. Comparisons of meters calibrated in different systems have shown the sensitivities obtained from calibrations in the Hatfield apparatus to be up to 75 per cent higher than those from R.A.E. calibrators.

(2) The maximum heat flow possible without generating excessive temperature is at least an order less than required.

(3) The time needed for calibration is too long; not more than one point per day could be produced.

(4) The requirement to calibrate heatmeters over a wide temperature range (−60 °C to +40 °C) could not be met.

5.3. *In situ* Calibrator

As the name given to it suggests the *in situ* calibrator (Fig. 11) was intended to be capable of being applied to a meter installed in a model and was thus as small as was considered practicable. It consisted of a cylinder, of

25·4 mm diameter, fitted with a spirally-wound single-layer heater at the top. This cylinder was surrounded by a guard heating arrangement and the whole of this was contained in an outer evacuated shell. The calibration technique employed was to place the calibrator over the heat-flow meter, which was embedded in the model or in a test piece representative of the model surface, and to hold the shell in contact with the surface. This was necessary initially because the cylindrical block was spring-loaded against the vacuum shell. However once the shell had been evacuated the assembly firmly attached itself to the model surface. In order to increase the uniformity of thermal conduction across the calibrator-meter interface, glycerine was used (a specifically-manufactured heat-sink compound not being available at the time). A further precaution taken was to blanket the remaining exposed surface with heaters and to match the resulting surface temperatures and also those of the guard heaters with the temperatures of the cylindrical block, in order to minimise heat losses, and to ensure as far as possible that a uniform heat flow passed through the meter and adjacent model surface. Heat was extracted by a coolant flowing through passages beneath the surface of the test piece or of the model.

This was the first calibrator used and as noted earlier gave sensitivities well below those quoted for commercial meters. In order to try and resolve this descrepancy the modified Lees disc calibrator was designed.

5.4. Modified Lees Disc Calibrator

This device, Fig. 12, was designed to calibrate individual heat-flow meters before installation into a model skin. An electrical heater is used as a source from which heat flows through the meter into a water jacket where a constant flow of water is maintained. The temperature difference of the water (ΔT) between inlet and outlet pipes is measured, enabling the heat flow out of the meter to be calculated for comparison with the heat supplied electrically. In order to maintain a one-dimensional heat flow through the calibrator a guard system, of similar thermal composition to the main stack, is used, enabling lateral temperature gradients to be minimised. During calibration it was found possible to keep the guard temperatures within $\pm 0{\cdot}5$°C of those at corresponding points in the centre stack. All thermocouple wires are routed along approximately isothermal paths to minimise heat flow along them

The entire assembly is placed in a bell-jar evacuated to 3 kPa with the electrical and water connections passing through a rubber plug. This level of vacuum (the best that could be obtained in this experiment) was thought at the time of making the tests to be sufficient to reduce the convection losses of the electrical heater to a negligible amount. However, it has since been demonstrated by Asteraki[22] that no significant difference in convection losses can be expected until the level of vacuum is below about 260 Pa. The effect of the convection losses may thus be the explanation for the discrepancy of 2·5 per cent between output and input power shown in Fig. 13. It should be noted that the maximum temperature difference obtained between the heater backing plate and room temperature was 70°C, whilst that between the water jacket and room temperature was about 3°C. The inaccuracies incurred due to the possible convection losses are small compared with the effect of reversing the meter which changed the calibration slope by about 7 per cent, although the relationship between input and output power remained the same. Unfortunately the measurements were plagued by inconsistencies of this kind in spite of the use of a heat sink compound (Midland Silicones Type DP 2623 in paste form) of similar thermal conductivity to that of the meters, smeared between the interfacing layers of calibrator and meter during each assembly.

The heater in this calibrator was a single layer resistance wire spirally wound to cover the whole cross-sectional area of the centre stack. In an earlier design use was made of a semi-conductor Peltier element as a heater, but this did not cover adequately the required area and it was more difficult to control the power accurately because of the relatively high currents involved, up to 15 A for the Peltier element compared with 0·8 A for the resistance wire heater.

5.5. Batch Calibrator

In an effort to speed up the calibration process a calibrator was made in which it was possible to mount twelve meters at a time (Fig. 14). This batch calibrator had a main stack diameter of 203 mm and the meters were fitted into pockets formed in a disc of the aluminium-resin material.

Repeatability in this device proved more of a problem than in the smaller calibrators because of the large area of the heat-flow field, and the consequent increased difficulty in maintaining uniform interfaces in the heat-flow path. It was not possible to measure the heat transmitted through the test disc because the cooling water removed the total heat input, including that to the guards. The pressure could be reduced only to 3 kPa and the same comments made in the previous section apply to the inadequacy of the pressure reduction.

5.6. Copper-block Comparator

There appeared to be two main problems in the use of the various calibration devices. One was the difficulty of maintaining good thermal contact with the faces of a heat-flow meter, and the other was the difficulty in ensuring that there was no stray heat paths. It was realised that perhaps these difficulties could be by-passed if an absolute calibration were not attempted. The calibration of the thermocouple heat-flow meters eventually chosen for the model depends upon three properties, the sensitivity of the thermocouples, their effective spacing, and the conductivity of the material in which they are imbedded. There was no reason to suppose that the material, which was prepared under strictly controlled conditions (see the Appendix), was not homogeneous and did not have consistent properties. The sensitivities of the thermocouples could be determined very readily, for example, by immersion in a stirred bath of fluid. Thus a calibration could be obtained if the effective spacing of the thermocouples could be found.

The simple device illustrated in Fig. 15 was therefore tried. This proved to give quick and repeatable readings. The way the device was used was to run cold tap-water, which was found to remain at a constant temperature for long periods of time, though the bottom tank. The upper copper block was warmed to a temperature about 15°C above the temperature of the tap-water by immersing it in a flask of hot water. The block was then placed on top of the meter which had heat-sink compound applied to the faces in contact with the copper blocks. The weight was then put on top of the copper block. Repeatable results were obtained provided the weight was at least 25 kg. (It was found that if the lower block was immersed directly in the tank some electrical leakage occurred from the thermocouple circuit and the thin sheet of mica was inserted to eliminate this.)

Temperatures were measured by thermocouples attached to the ends of the copper blocks near the upper face of the lower block and near the lower face of the upper block, and also by the thermocouples in the heat-flow meters. Fig. 17 shows the variation of the difference in temperature indicated by the two thermocouples fitted in a selection of heat-flow meters, plotted against the difference in temperature between the two copper blocks, as the upper block was allowed to cool. As can be seen there is a linear relationship between the two temperature differences. The slope of the line drawn can be taken as indicating the ratio of the separation of the thermocouples to the thickness of the meter, since the thermal conductivity of copper is about 400 times that of the resin mixture. The values of the slopes for the four meters shown in Fig. 17 range between 0·7 and 0·85. It was found that the slopes were within about ± 2 per cent for repeated testing of the meters mounted both in the forward and reverse directions.

Because of the consistency of the results obtained from it, and because of the convenience and speed with which measurements could be made, the comparator became the standard device in which most of the heat-flow meters for the model were tested. Absolute values for sensitivity were obtained by reference to meter No. 17 which had been checked in other calibrators and had a well-substantiated absolute calibration. A further comment on the use of the device as a means of calibrating the 'surface-temperature thermocouple' is given in Section 6.

5.7. Single-path Calibrator

This device, Fig. 16, has been described by Asteraki[22] and was designed to minimise the number of parallel heat flow paths present in other apparatus. The main heat-flow bar has the same cross-sectional area as a heat-flow meter to be calibrated. The calibrator operates with a heat flow vertically downwards. Heat is supplied electrically at the top of the copper bar and flows through the meter, to be removed by liquid coolant at the bottom. A system of guard heaters is incorporated to minimise losses, and the main chamber may be evacuated to a sufficiently low pressure to eliminate convection effects. It is not intended that this calibrator will be used for large numbers of calibrations because of the length of time required to rig and calibrate each meter, but it provides a standard for assessing other methods of calibration or for testing new forms of heat-flow meters. It is envisaged that it will be used in conjunction with the copper-block comparator to calibrate batches of heat-flow meters for future models.

Altogether four meters, of separate bead thermocouple design, which had already been calibrated in both the modified Lees disc and the batch calibrator, have been calibrated in this device. For three of these, well-behaved calibrations were obtained and the results are compared with those from other calibrations in Table 2. The fourth meter gave a very low value of sensitivity compared with that obtained in other calibrators and also had a non-linear calibration. It was assumed that a defect had developed in the meter and it was not used subsequently.

6. Discussion of Performance of Heat-Flow Meters

As stated previously, the heat-flow meters chosen for the wind tunnel model were the separate bead thermocouple meters. Although in principle these were ten times less sensitive than the semiconductor type, they could be made to a much closer tolerance, their calibrations appeared to remain stable, and a measurement of nominal surface temperature could be made.

Relative calibrations of 121 meters of this type were made using the copper-block comparator. Typical results are given in Fig. 17, and a histogram showing the distribution of sensitivities for all meters in Fig. 19. An absolute calibration was attributed by comparison with meter No. 17 which had behaved well in both the modified Lees disc and batch calibrators and had a sensitivity of 50 μV kW^{-1} m^2.

Unfortunately, in general, little confidence was possible in the absolute calibrations because of variations in sensitivity when a meter was inverted or indeed removed and replaced. It is felt that most of the problems can be attributed to the interfaces between various layers of the calibrators and in particular between the heat-flow meter and its surrounding heat path. This problem was particularly acute on the batch calibrator where the large mounting disc was particularly susceptible to distortion. Calibrations for the disc mounted in upright, inverted or rotated positions were markedly different.

A comparison of the results for six separate bead thermocouple meters from four different calibration devices is shown in Table 1 where the sensitivity for a particular meter can be seen to vary by as much as 28 per cent.

TABLE 1

Meter	Sensitivities in μV kW^{-1} m^2 using various calibrators				% variation
	* Copper block	Modified Lees disc	Batch calibrator	Asteraki calibrator	
17	50	50	50·4	—	0·8
25	56	46·4	54·4	62	28
74	53	50	49·5	—	6·9
136	57	56	51·1	55	10·8
145	57·8	47	45·9	—	24
148	49·7	—	—	63	24

* Absolute figures obtained using meter 17 as datum.

An estimate for the sensitivity can be obtained from a knowledge of the properties of the thermocouples and of the encapsulation material. As shown in Fig. 20 the thermal conductivity of the aluminium-resin mixture varies from 1·05 W m^{-1} °C^{-1} at a temperature of −60°C to 1·07 at a temperature of +40°C. The meter thickness is 1·52 mm and the thermocouple sensitivity varies linearly from 37·2 μV °C^{-1} at −60°C to 42·2 μV °C^{-1} at +40°C. These figures lead to values of heat-flow meter sensitivity varying from 54 to 60 μV kW^{-1} m^2 over the temperature range −60°C to +40°C. The value at room temperature at which most of the calibrations were made is 58 μV kW^{-1} m^2. The average measured value of about 52 (Fig. 19) thus suggests that the effective spacing of the thermocouple beads is about 1·36 mm, rather than the full thickness of the material, 1·52 mm. The fact that two of the values of meter sensitivity obtained from the Asteraki calibrator are higher than the estimate has not been explained. The effective spacing would appear to be roughly the distance between the centres of the beads as seen in Fig. 10. The temperature sensed by the surface-temperature thermocouple will therefore be that at a depth about 0·08 mm below the surface. In practice the effect of the required correction to measured Stanton number is small since the temperature difference across the heat-flow meters is small compared with $T_w - T_r$. An analysis of the measurements taken in the copper-block comparator was, however, made in an attempt to derive a direct assessment of the effective depression of the particular thermocouple to be used to measure surface temperature in each heat-flow meter. A sample of the results is given in Fig. 18a. The slopes of the plots of temperature difference between the surface thermocouple and the adjacent copper block, against the temperature difference between the copper blocks, varies from about 0·2 to 0·06, implying depressions of the thermocouples between 0·3 and 0·09 mm.

These estimates assume that any thermal resistance in the copper blocks or the interfaces to the meters may be neglected. This assumption may be the main reason for the large values of the depression measured, as compared with that predicted from the properties of the materials. It is, however partially justified by the relatively good agreement between the two sets of measurements with the meters upright and inverted. The alternative presentation of Fig. 18b shows the calibration in the form used to evaluate the results of the tunnel test on the model.

The variations in sensitivity between meters are thought to be due primarily to geometrical differences in mounting of thermocouple beads, that is their effective spacing and the routing of their wires (Fig. 10). Other factors contributing are minor differences in the thickness of the block and possible variation in its thermal conductivity due to the presence of air bubbles in the mixture, although X-ray photographs failed to show this. As can be seen in Fig. 5 the meters in the model are mounted principally in transverse rows. From the 121 meters available the 71 with sensitivities closest to the mean were chosen, the variation being ± 14 per cent. They were arranged so that the variation of sensitivity for meters in a given row is less than $\pm 2\frac{1}{2}$ per cent.

Some indication of the response of a heat-flow meter to a change in conditions is given in Fig. 21. The ratio of the voltage signal from the lower thermocouple to its final value is shown with respect to time. These results were obtained using the *in situ* calibrator placed over a meter in the model, with coolant flowing through the model. The response was obtained by making a step change in the powers supplied to the calibrator. Two sets of data are shown and are well represented by an exponential decay curve

$$\frac{V}{V_0} = 1 - e^{-0{\cdot}8t}. \tag{11}$$

A settling time of 5 minutes would thus appear to be appropriate to give an accuracy of better than 0·7 per cent.

7. Test Experience

To obtain reliable measurements of the heat transfer to a model in a wind tunnel under steady-state conditions requires accurate control of the model temperature, and precise instrumentation. The main need is to establish steady surface temperatures so as to eliminate the effect of changing temperatures on the apparent heat flow through the model. To meet this requirement the coolant inlet temperature and coolant flow to the model should be maintained constant over a sufficient period of time to allow steady heat flow to become established in the model, and to permit the required data to be recorded.

7.1 Model Instrumentation

It is necessary to measure accurately the temperature on the two sides of each heat-flow meter. The upper temperature is used, via calibrations of the kind shown in Fig. 18, to derive the model surface temperature, and the difference in temperature is a measure of the heat-flow rate. The differencing was done electrically as shown in Fig. 22.

The copper leads from the thermocouples were fed to two 72-way low-level solenoid-operated switches, allowing the surface temperature and temperature difference for the meters to be recorded at the same instant, and in a prescribed sequence. The temperatures were referred to a thermocouple junction which was kept at 0°C in a vacuum flask containing water and melting ice. The constantan leads from the thermocouples were welded to a common bus bar at the trailing edge of the model, and a single uninterrupted constantan cable consisting of seven strands of 0·275 mm wire was led to the reference junction. Care was taken in the selection of a stout constantan wire for the bus bar and the connecting cable to the reference junction to avoid the spurious voltages which have been obtained when a constantan–constantan junction has been formed between two randomly acquired wires; up to 7 per cent of the voltage produced by a copper–constantan junction has been measured.

The pressure tubes passed to the rear of the model within the steel shell and then to a 72-way pressure-scanning switch containing an unbonded–strain-gauge pressure transducer. The pressure switch contains extra ports between those used for measurement, to allow a given pressure to be applied to the transducer between measurements to minimise hysteresis effects.

The signals from the pressure transducer and the heat-flow meters were each measured by a potentiometric chart recorder containing a digitiser connected to a card punch. The recording system, Fig. 22, was capable of resolving 1 μV on the most sensitive range (1 mV fsd). Most of the data for the heat-flow meters were recorded on the 4 mV fsd range which gave a resolution of 0·1°C for temperature and about 80 W m^{-2} for heat transfer.

At the rear of the model the instrumentation was shielded from the airflow by means of a pair of fibreglass fairings which may be seen in the photograph of the model (Fig. 6). The fairings were bolted to the sting mounting which supported the model, and were moulded around the coolant pipes and screwed together at the edges. The upstream edges of the fairings were chamfered so that they could be positioned close to, but recessed below, the trailing edges of the model to leave a 'clean' airswept surface.

7.2. Coolant Instrumentation and Testing Procedure

A semi-automatic system was devised to control the model coolant temperature. During a test the temperature of the mixing tank (see Fig. 2) was reduced to a temperature below that desired at the inlet to the model. The procedure adopted was to adjust the control valves manually so that the temperature of the flow from the heat exchanger was slightly less than that required at the model inlet. The coolant was pumped to the model through the 6 kW electrical heater. Immediately downstream of the heater a temperature-control sensor was inserted into the circuit. The sensor was a platinum resistance element which formed one arm of a Wheatstone bridge. The out-of-balance voltage was sensed by an Ether control unit which switched the heater on or off. The opposite arm of the bridge to the sensor contained a decade resistance box which was set so that the bridge would balance when the resistance of the platinum element was compatible with the required inlet coolant-temperature. A variable auto-transformer in series with the heater allowed its power to be trimmed, so providing an optimum heating rate. By judicious control of the heater power, and of the temperature of the coolant flow from the heat exchanger, so that it was slightly cold relative to the Ether control-unit setting, it was possible to minimise the swing of temperature of the inlet flow.

The model inlet temperature was measured at the model inlet port with another platinum-resistance thermometer, the output of which was displayed on an $x-t$ chart recorder. Thus the model-inlet coolant-temperature could be monitored, and it was found possible, under ideal conditions, to maintain it constant to within 0·02°C for periods up to 10 minutes. Three sample records of the model-inlet coolant-temperature are shown in Fig. 23. These records are for nominal inlet coolant-temperatures of −56, 20 and 40°C. The arrows show where changes were made to the model attitude, and it can be seen that these changes produced step changes in inlet temperature. The likely cause of these step changes is a variation in the pressure drop in the coolant circuit caused by distortions of the flexible supply pipes to the model. The variations in pressure drop cause changes in the flow through the coolant circuit, causing, in turn, changes in the temperature difference between the point at which temperature is controlled and the model inlet. The effect might have been avoided by using the temperature sensor at the model inlet for control. However, in order to obtain both a quick response and good stability it was found necessary to place the control sensor immediately adjacent to the heater and thus at some distance from the model. As may be seen in Fig. 23, for the examples given for inlet temperatures of −56 and +20°C, there are also slight drifts of temperature with time. These may be associated with long term changes of the total temperature of the tunnel air and of the temperature of the tunnel structure. These changes in temperature will modify the heat transfer from the coolant supply pipes within the tunnel shell and result in a drift in coolant temperature at the model inlet for a constant temperature at the control point. The procedure adopted to obtain reliable readings in spite of the temperature changes and drifts was to allow a settling time of at least five minutes after a change in model attitude, followed by a check on the constancy of the coolant temperature before recording the data. A further recording was taken afterwards to ascertain whether any drift was apparent during the period of data acquisition.

The time required to change the coolant temperature depended upon the direction of the temperature change. The maximum rate of heating was 0·5°C per minute, limited by the power available from the electrical heater. The maximum cooling rate was 2°C per minute, limited by the highest flow rate of the coolant and the temperature of the coolant in the mixing tank. The flow rate through the model was limited by the maximum safe inlet pressure of 415 kPa.

7.3. Data Reduction

Some preliminary results obtained on the model are described in Section 3.2 at a Mach number of 2·45, and a Reynolds number, based on root chord, of $1{\cdot}3\times10^7$, are discussed in Sections 7.4 and 7.5. The parameters required to describe the aerodynamic heat transfer are the recovery temperature, T_r, that is the surface temperature which gives zero heat transfer, and a Stanton number

$$\mathrm{St}=\frac{h}{\rho_\infty u_\infty C_p(T_w-T_r)} \tag{12}$$

where

h = rate of heat transfer per unit area
ρ_∞ = freestream air density
u_∞ = freestream velocity
C_p = specific heat of air at constant pressure
T_w = wall temperature.

The recovery temperature, T_r, was obtained by interpolating, at zero heat transfer rate, the surface temperature measured for a range of cooling and heating flows. The heat transfer rate, h, and the wall temperature were obtained from the individual calibrations of the heat-flow meters.

This simple method of data reduction neglects any effects arising from the transverse flow of heat. For meters of the twin-thermocouple type, used in a suitable array, approximate corrections can be made for lateral conduction. Consider a model wall as being locally represented by a rectangular slab of material of thickness l, and take axes z normal to the slab and x, y in the plane of the inner surface of the slab. Within the slab the temperature distribution is governed by Laplace's equation

$$\frac{\partial^2 T}{\partial x^2}+\frac{\partial^2 T}{\partial y^2}+\frac{\partial^2 T}{\partial z^2}=0. \tag{13}$$

Therefore, if the heat-flow meters are arrayed say with five meters in a cross-formation, $\partial^2 T/\partial x^2$ and $\partial^2 T/\partial y^2$ can be obtained approximately for the centre point at both surfaces of the slab, and hence $\partial^2 T/\partial z^2$ can also be obtained from (13). The temperature distribution through the slab can therefore be represented locally by a third-order polynomial in z satisfying the conditions

$$\begin{aligned} &z=0, \quad T=T_b, \quad \frac{\partial^2 T}{\partial z^2}=-\left(\frac{\partial^2 T}{\partial x^2}+\frac{\partial^2 T}{\partial y^2}\right)_b=T''_b \\ &z=l, \quad T=T_w, \quad \frac{\partial^2 T}{\partial z^2}=-\left(\frac{\partial^2 T}{\partial x^2}+\frac{\partial^2 T}{\partial y^2}\right)_w=T''_w. \end{aligned} \tag{14}$$

Hence

$$T=T_b+\frac{T_w-T_b}{l}z-\left(\frac{T''_w}{6}+\frac{T''_b}{3}\right)lz+\frac{T''_b}{2}z^2+\frac{T''_w-T''_b}{6l}z^3$$

and the heat flow at the wall

$$h=k_s\left(\frac{\partial T}{\partial z}\right)_w=\frac{k_s}{l}(T_w-T_b)+k_s l\left(\frac{T''_b}{6}+\frac{T''_w}{3}\right). \tag{15}$$

The first term in (15) is the one-dimensional term directly from the calibration and the second term is a correction for lateral conduction. The effective thickness and thermal conductivity of the wall are required for its evaluation. For the results shown in Figs. 24 and 25 the correction to Stanton number did not exceed 1 per cent.

An alternative experimental arrangement is considered by Piggott[23] in which the quantities determined are the temperature of the outer surface and the heat flow at the inner surface. He describes a finite-difference computer program to solve the problem of finding the heat transfer at the outer surface for two-dimensional conditions.

7.4. Results $\alpha = 0°$

Fig. 24 shows two sample sets of data at zero angle of incidence for the row of heat-flow meters close to the ridge line. The results shown are for model-inlet coolant-temperatures of +40 and −56°C. It is apparent that the objective of constant surface temperature was not achieved. There two reasons for this. Firstly, because of the thin section at the leading edges and near the nose, it was not possible to cool these regions effectively, and, as can be seen from Fig. 24, the surface near the nose remains at about recovery temperature. Secondly, the coolant flow in the pipe arrangements within the model was not uniform because of variations in flow rates in

individual pipes, despite the adjustment provided by the needle valves, probably as a result of corrosion or sediment in the pipes. The disturbance in temperature near $x/c = 0{\cdot}65$ is attributed to maldistribution of coolant flow in the aft bank of cooling tubes (Fig. 3). The plots of measured Stanton numbers in Fig. 24 are compared with estimates made by two available calculation methods. The full line is from the method of Verma[24] which uses a finite-difference eddy-viscosity model, and the broken line is from the lag-entrainment method of Green *et al.*[25]. In making the calculations the measured surface temperature was used, together with the local Mach numbers estimated from the measured pressures. The local Mach number was in fact about 2·32. The model was fitted with a transition trip of Ballotini of 0·5 mm diameter close to the leading edges. The calculations were started by assuming an adiabatic flat-plate turbulent boundary layer to develop from the leading edge up to the point where the momentum thickness Reynolds number reached a value of 1000, when the detailed calculations were begun. The calculation methods agree with each other within 10 per cent, and the scatter of the measured points about the calculations is within about ±15 per cent. The calculations illustrate the perturbations to the Stanton number distribution caused by the streamwise changes in surface temperature. In particular the tendency for a minimum to occur at x/c between 0·6 and 0·7 is a result of the temperature changes. For the cold run, for example, the surface temperature upstream of this region is relatively low, and consequently the temperature of the air approaching the region is lower than it would have been for an isothermal surface, and a reduced Stanton number occurs. Downstream of $x/c = 0{\cdot}7$ the surface temperature ceases to increase and consequently the Stanton number rises above the minimum value.

7.5. $\alpha = 10°$

Some results with the model at an angle of incidence of 10° and with angle of sideslip β varying from +14 to −14° are shown in Fig. 25 for the row of heat-flow meters at two-thirds root chord. The coolant rate was the maximum obtained, with the inlet coolant-temperature at about −56°C. The Stanton numbers have been normalised with respect to the Stanton number obtained at zero incidence and zero sideslip with the same coolant temperature. Corresponding pressure coefficients are shown in Fig. 26.

At this angle of incidence the flow separates from the leading edges of the model as it does from the leading edges of a slender wing at low speeds. At supersonic speeds the effects of the separation on the boundary-layer flow are, however, different and the changes in character of the separation with change in angle of sideslip are also different. The low-speed experiments of Wyatt and East[26] on the skin friction, at zero angle of sideslip, on a model similar to that of the present tests, show that the spanwise distribution of skin friction is related closely to the pressure distribution. There is a maximum in c_f on the locus of the streamline inflection points which corresponds roughly to the position of the peak suction, and a minimum in c_f further outboard at the position of the secondary separation. The attachment line, which is roughly at the position of the pressure maximum, appears to have no special significance as far as c_f is concerned. However at supersonic speeds[27] the behaviour is different, with a peak in skin friction occurring at what might be surmised to be the attachment line and with a minimum at the position of peak suction. Some of this difference in behaviour may be ascribed to the different way in which kinetic pressure changes with static pressure at supersonic speeds and also to the extra influence of Mach number changes associated with pressure changes. At low speeds the effect of sideslip on a delta wing with separated flow is to increase the strength of the vortex on the windward edge and to increase the level of suction there, with the opposite happening on the lee side[28]. The behaviour of the separations at supersonic speeds is different, mainly because the Mach number normal to the leading edge is an important variable. For the present model for example for $\beta = -14°$ the Mach number normal to the port leading edge (the measurements were made on the port half of the wing) has a value of 1·15 and it is thus unlikely that there is extensive separation there. That is, there is a reduction in the strength of the vortex on the windward edge. This is confirmed by the pressure and heat transfer measurements which both have relatively little variation. The variation of the heat transfer appears broadly to be related to the pressure distribution in the same way as the skin friction and pressure distribution were related on a similar model, but at zero angle of sideslip, in reference 27. Regions of high suction lead to low values of heat transfer and a maximum in heat transfer occurs near the maximum pressure. The largest region of separation appears to occur for $\beta = -5°$ and this angle of sideslip also leads to the largest variation in heat transfer. At this condition the ratio of Stanton number to that at zero angle of incidence varies over a range of 5:1 across the spanwise station considered. This large variation could have important implications in the design of slender aircraft to fly at supersonic speeds.

8. Future Lines of Development

From the extensive work needed both in the design and manufacture of the model described, and in the development of the heat-flow meters, it is clear that the techniques for measuring heat transfer under

steady-state conditions in the R.A.E. wind tunnels require considerable further development. The method of construction of the model is too complex for all but the most simple shapes, and is fraught with pitfalls even then. Some further work was undertaken to investigate other means of manufacture and a design was prepared for a model of Concorde. For various reasons however, the model was not made.

An alternative approach was adopted to the design of the coolant passages beneath the model skin. As noted in Section 3.1, the passages must be small in order to obtain a sufficiently high rate of heat transfer to the coolant with the limited flow available; adequate heat transfer will not be obtained simply by producing chambers within the model. The alternative approach was to provide machined passages in the model shell instead of attaching pipes to the shell. The shell was to be made of stainless steel to avoid the corrosion problems of the present model. An attractive means of closing the passages appeared to be the use of the electrodeposition process. Test pieces were made to examine this possibility. Channels, representing coolant passages, were machined in a block of stainless steel. The channels were then filled, either with a low melting-point alloy or by means of an aluminium spray, and the surface machined again so as to be flat. A skin of nickel was then formed over the surface by electrodeposition, and the filler in the channels either melted out or removed by a caustic agent. The nickel skin, which was about 5 mm thick, was intended to form the outer surface of a model on to which a resin surface would be cast. The heat flow would be measured by gauges in the resin skin as in the present model. The test pieces highlighted two major problems. The first of these was that it appeared impossible to obtain adhesion between the deposited nickel and the stainless steel. The reason for this was considered to be the stresses which built up in the nickel skin as its thickness grew. Some attempts were made to bond the two materials after the deposition process by electron-beam welding but the results were unreliable, and the method would have been extremely difficult and expensive on a complicated model. It was concluded, therefore, that if the deposition process were used then, as far as possible, adjacent coolant passages should be matched in respect of coolant flow and pressure-drop characteristics, so that some communication between the passages would not be of great consequence. Some mechanical fixings would however have been required to prevent distortion of the skin because of the high pressure required to circulate the coolant. However, the scheme was condemned by the second main problem; that of obtaining adhesion of epoxy resin to nickel. No satisfactory way of achieving this was found and the design was abandoned. The design finally adopted used a machined stainless steel skin attached mechanically (by screws) to the channelled shell. Because no gasket material could be found which would be unaffected by exposure over long periods to trichloroethylene, the passages were designed to have metal-to-metal seals only and were intended to be matched, as suggested above, in respect of coolant-flow characteristics. With regard to heat-flow meters it is obviously highly desirable to avoid the tedious and unreliable calibration process both for the heat flow and for the measurement of surface temperature. This could be done by using either thin-film resistive elements or thin-film thermocouples on either side of a material of known thermal conductivity. Thermocouples would be preferred, as being active elements, and advances in sputtering techniques[20] indicate that their manufacture can now be undertaken. Their use would lead to some freedom in the choice of the skin material and some further investigation is needed to determine materials which would have the required thermal characteristics, be suitable as a substrate for sputtering, be capable of withstanding the thermal stresses imposed in practical applications, and be capable of being bonded to whatever material eventually proves most satisfactory for the shells of models.

Acknowledgments

The authors have great pleasure in acknowledging the efforts and close cooperation of the staff of the (then) Ministry of Public Buildings and Works and of their contractors Messrs. CJB in the design and manufacture of the cooling plant, and of the staff of Messrs. TEM Engineering Ltd. in the design and manufacture of the model. Thanks are also due to the staff of the Basic Physics Division of the National Laboratory who measured the values of thermal conductivity quoted.

LIST OF SYMBOLS

a_a, a_c, a_s	Effective conductivities (see equations (4), (5) and (6))
c	Local chord of model
C_p	Specific heat of air at constant pressure or specific heat of coolant or pressure coefficient
d	Pipe diameter
h	Rate of heat flow per unit area
k	Thermal conductivity
l	Thickness of skin or of heat meter
m	Mass flow in pipe $= \frac{1}{4}\rho u \pi d^2$
N	Number of tubes
Nu	Nusselt number
Pr	Prandtl number
Re	Reynolds number
R	Radius of Gardon-type meter
s	Mean span of model
S	Local span of model
St	Stanton number (see equation 12))
t	Time in minutes
T	Temperature
u	Velocity
V	Voltage
V_0	Final voltage
x	Chordwise distance
y	Spanwise distance
z	Distance from inner face of skin
α	Angle of incidence
β	Angle of sideslip
ΔT	Temperature difference
ρ	Density
μ	Viscosity
σ	Standard deviation

Subscripts

0	Refers to total temperature conditions
1	Refers to upper thermocouple
2	Refers to lower thermocouple
b	Refers to bottom of skin
c	Refers to coolant
l, u	Refers to lower and upper copper blocks (see Fig. 15)
r	Refers to recovery conditions
s	Refers to skin
w	Refers to wall conditions

REFERENCES

No.	*Author(s)*	*Title, etc.*
1	D. L. Schultz and T. V. Jones	Heat-transfer measurements in short-duration hypersonic facilities. AGARDograph No. 165 (1973).
2	C. M. Howard and H. T. Wood, Jr. ..	Mechanical design of the 50-inch Mach 10–12 tunnel. AEDC-TDR-229 (1963).
3	J. C. Sivells	Operational experience with a 50-inch diameter Mach 8 tunnel. STA-AGARD Wind-Tunnel and Model Testing Panel Meeting Marseille (1959).
4	A. Naysmith	Measurements of heat transfer in bubbles of separated flow in supersonic air streams. R.A.E. Technical Memorandum Aero 709 (1961). Proceedings of the 1961–62 Heat Transfer Conference University of Colorado pp. 378–381 (1961).
5	W. H. McAdams	*Heat transmission.* McGraw-Hill (1954).
6	H. Stafford Hatfield and F. J. Wilkins	A new heat flow meter. J. Sci. Inst., Vol. 27, 1, 1–3 (1950)
7	J. Plenier	Notes of a thermal fluxmeter. Etablissement Aéronautique de Toulouse. R.A.E. Library Translation 843 (1958).
8	R. Gardon	A transducer for the measurement of heat flow rate. Trans. Am. Soc. Mech. Engrs. 2, p. 396 (1960).
9	E. W. Northover and J. A. Hitchcock	A meter for the determination of local heat transfer coefficient. The Institution of Mechanical Engineers, Thermodynamic and Fluid Mechanics Convention Cambridge. Proc. Instn. mech. Engrs., Vol. 178, Part 3 I(i) (1963–4).
10	L. L. Trimmer, R. K. Matthews and R. D. Buchanan	Measurement of aerodynamic heat rates at the von Karman facility. Proceedings ICIASF CIT 35–44, 10–12 September 1973.
11	N. E. Hager	Thin foil heatmeter. Rev. Scient. Instrum., pp. 1546–1570 (1965).
12	E. H. Schulte and R. F. Kohl	Low temperature high sensitivity temperature compensated heat flux sensor. Rev. Scient. Instrum, Vol. 40, 11, 1420–1427, November 1969.

13 E. H. Schulte and R. F. Kohl ..... A high heat flux sensor employing semi-conductors.
Int. Cong. on Instn. in Aerosp. Sim. Fac. ICIASF 69 Record 269–277.

14 E. A. Laumann ..... A steady state heatmeter for determining the heat transfer rate to a cooled surface.
Jet Propulsion Labs., Cal. Inst. Tech. Technical Memorandum 33–120 N63 18868 (1963).

15 F. W. Hartwig, C. A. Bartoch and H. McDonald Miniature heat meter for steady-state aerodynamic heat transfer measurements.
J. Aero Sci. Readers Forum p. 239 (1957).

16 F. W. Hartwig ..... Development and application of a technique for steady state aerodynamic heat transfer measurements.
Cal. Inst. Tech. Hypersonic Res. Proj. Memo 37 (1957).

17 D. R. Hornbaker and D. L. Rall .... A practical guide to heat transfer measurements.
Paper No. P11-1-PHYMMID-67, 22nd Annual ISA Conference Proceedings, Part II (1967).

18 D. L. Johnson ..... The design and application of a steady state heat flux transducer for aerodynamic heat transfer measurements.
ISA Transactions, Vol. 4, 1, pp. 46–53 (1965).

19 C. H. Bryce and V. H. R. Hole ..... Measurement and control by thermistors.
Industrial Electronics pp. 294–296 (1967).

20 S. C. Metcalf and S. G. Dumbrell ... New methods of preparation of thin film gauges for surface heat transfer and temperature measurement.
Paper presented at Euromech 24, Prague, April 1971.
R.A.E. Technical Report in preparation.

21 D. L. Rall and F. C. Stempel ..... A discussion of the standardised procedure for calibrating heat flow transducers.
19th Annual ISA Conference Proc., Vol. 19 II. Preprint 16 (1964).

22 D. L. Asteraki ..... A calibration apparatus for heat-flow transducers.
R.A.E. Technical Report 70100 (1970).

23 B. A. M. Piggott ..... A method for correcting measurements of the heat transfer factor through the skin of a wind tunnel model.
A.R.C. C.P. 860 (1964).

24 V. K. Verma ..... A method of calculation for two-dimensional and axisymmetric boundary layers.
Univ. of Cambridge Dept. of Engr.
CUED/A Aero/TR3 (1971).

25 J. E. Green, D. J. Weeks and D. W. Brooman — An integral prediction method for turbulent boundary layers with heat transfer, based on a simple polar of temperature against velocity.
Paper presented at Euromech 43, Gottingen, May 1973.
R.A.E. Technical Report in preparation.

26 L. A. Wyatt and L. F. East ..... Low speed measurements of skin friction on a slender wing.
A.R.C. R. & M. 3499 (1966).

27 K. G. Smith, L. Gaudet and K. G. Winter — The use of surface pitot tubes as skin-friction meters at supersonic speeds.
A.R.C. R. & M. 3351 (1962).

28 J. K. Harvey ..... Some measurements on a yawed slender delta wing with leading-edge separation.
A.R.C. R. & M. 3160 (1958).

APPENDIX

Preparation of the Material for the Skin of the Model

During work on tellurium–silver heat-flow meters, potting compounds were investigated with the aim of finding an encapsulation material with similar thermal properties to the semiconductor material. It was decided that the whole of the heat transfer model outer skin (1·52 mm thick) should be made of this material so that the heat flow through the skin would not be disturbed by the presence of the semiconductor element. Further work was carried out by TEM Engineering Ltd., to find a suitable formula to achieve both a good thermal match and also a satisfactory bond between this layer and the steel shell of the model which would not crack as a result of the temperature variations (−60 to +40°C) to which it would be subject. Basically the material used was an epoxy-resin loaded with aluminium powder ($k = 1$ W m^{-1} °C^{-1}). The substrate of all meters tested was of this material for which the formulation is:

60 parts Shell resin 828	
20 parts synolide 950	
20 parts versamid 140	all parts by weight
100 parts aluminium powder	
170 mesh to dust	

Before mixing, the components were individually pre-heated to 70°C for about 30 minutes, then the Shell resin 828 was mixed with the aluminium powder and placed in a vacuum vessel in which the pressure was reduced to about 6 kPa whilst the mixture was agitated to release trapped air bubbles. A similar procedure was followed with the remaining ingredients which were individually subjected to vacuum. The ingredients were then allowed to return to room temperature after which they were all mixed together and a vacuum applied once more. The cure procedure consisted of pouring the mixture into a mould, leaving at room temperature for 30 minutes then baking in the oven at 75°C for $2\frac{1}{2}$ hours.

The rubberised sub-layer used between the outer skin and the steel shell was formulated as follows:

12 parts BPI resin PR905/1 part A	
11 parts BPI resin PR905/1 part B	all parts by weight
25 parts aluminium powder 170 mesh to dust	

A procedure similar to that used for the outer skin was followed for preheating and subjecting the ingredients to vacuum, followed by a similar cure.

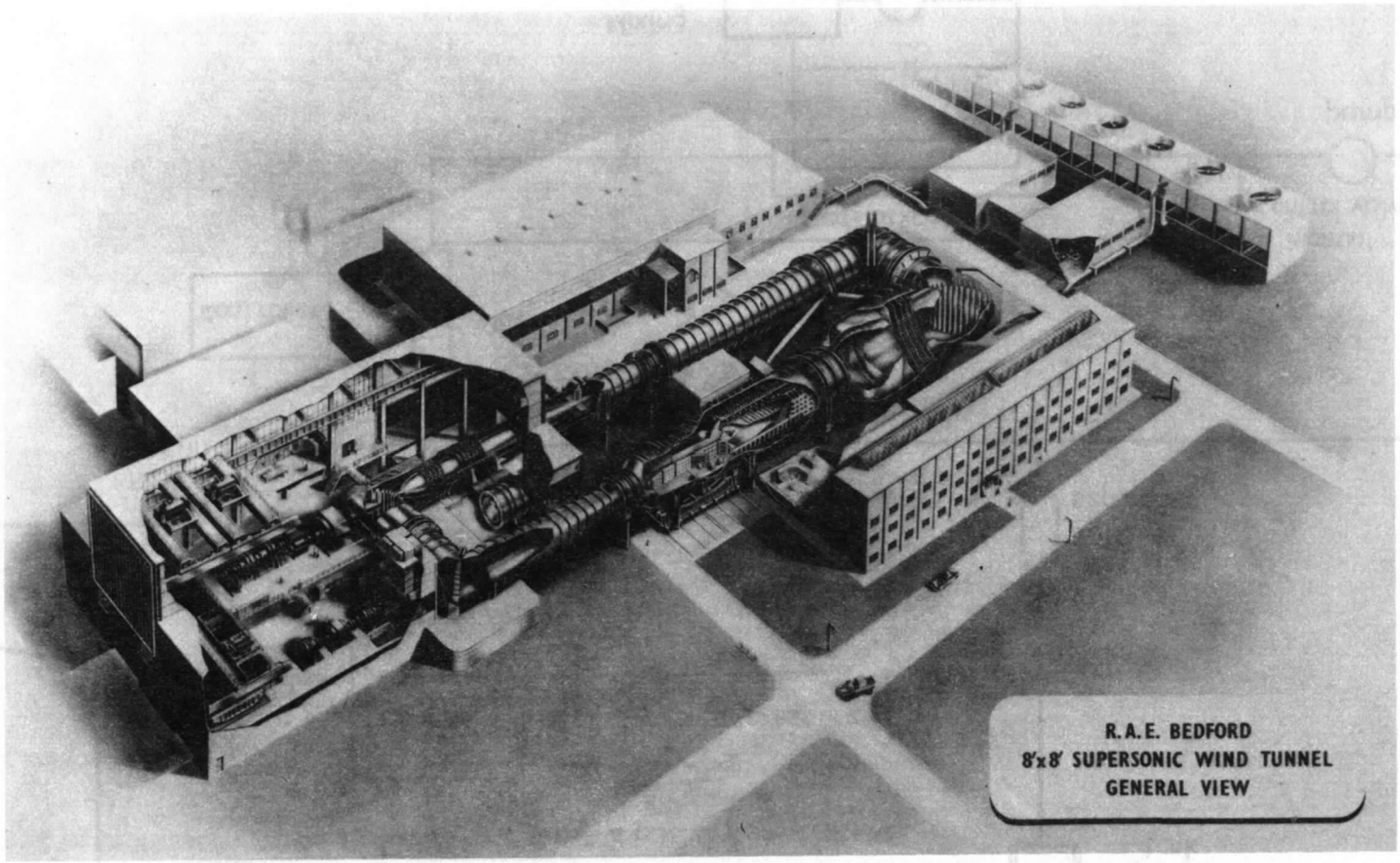

FIG. 1. R.A.E. Bedford 8 ft × 8 ft supersonic wind tunnel—general view.

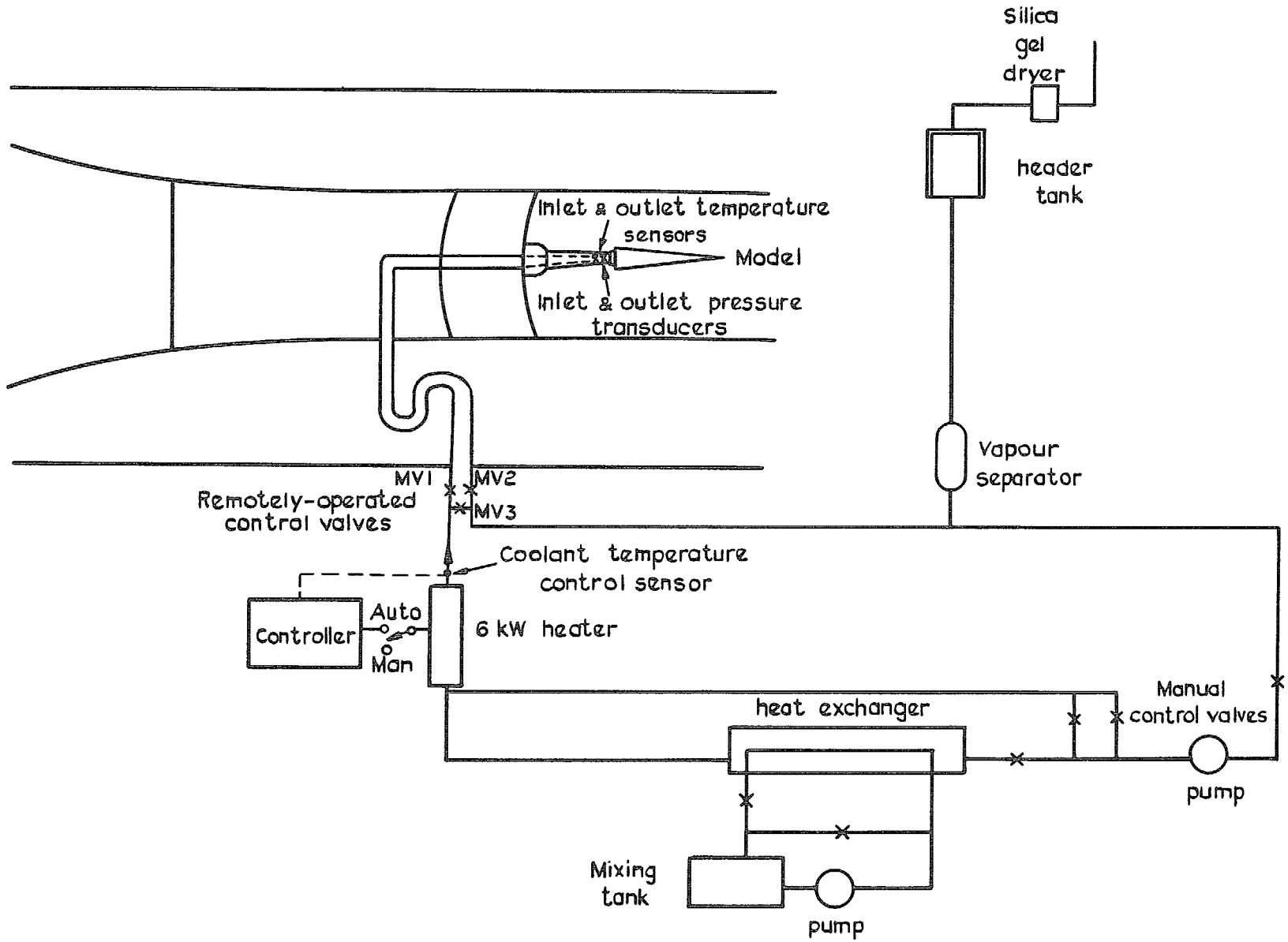

FIG. 2. Model cooling system.

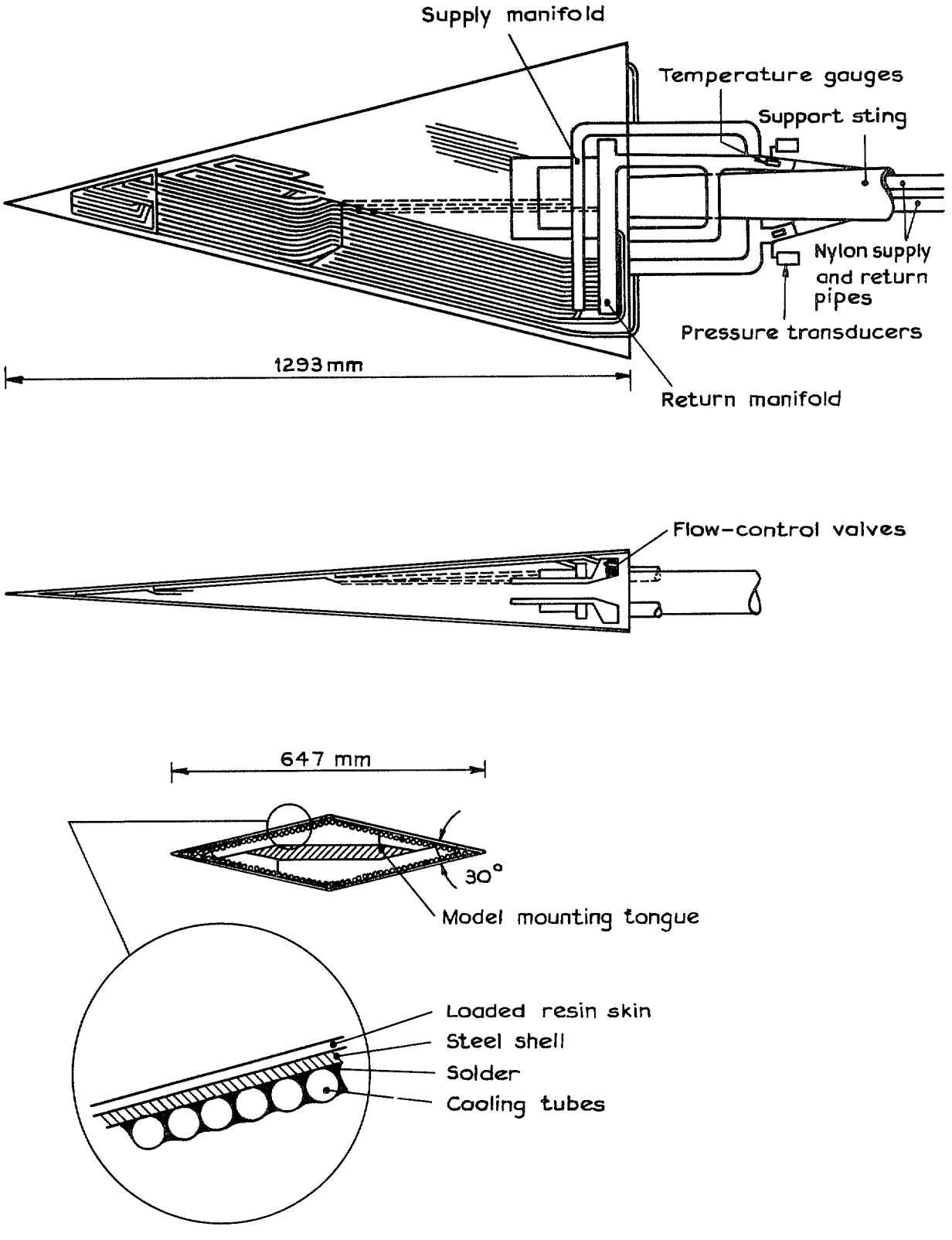

FIG. 3. Arrangement of model.

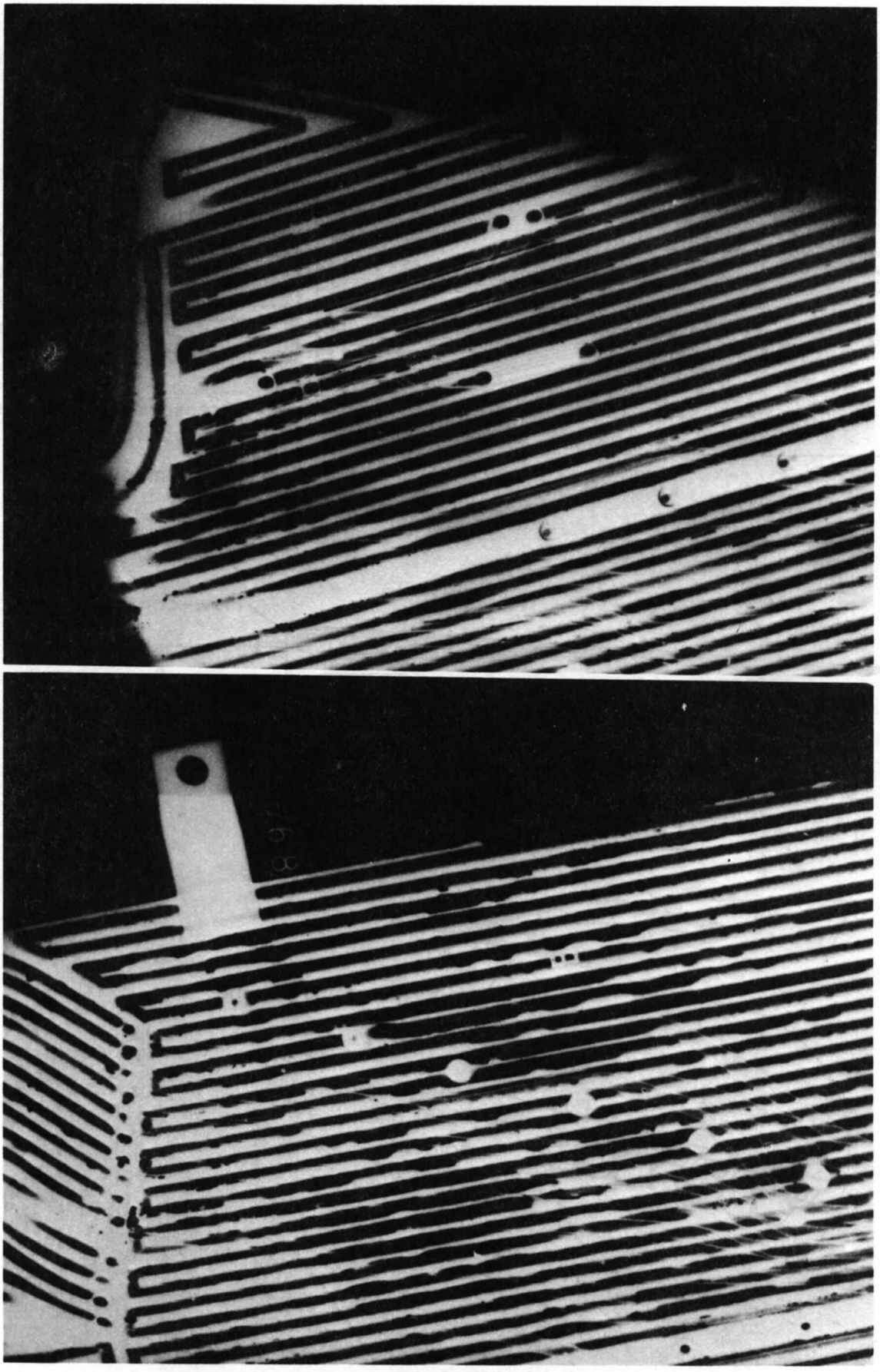

FIG. 4. Examples of good and bad soldering.

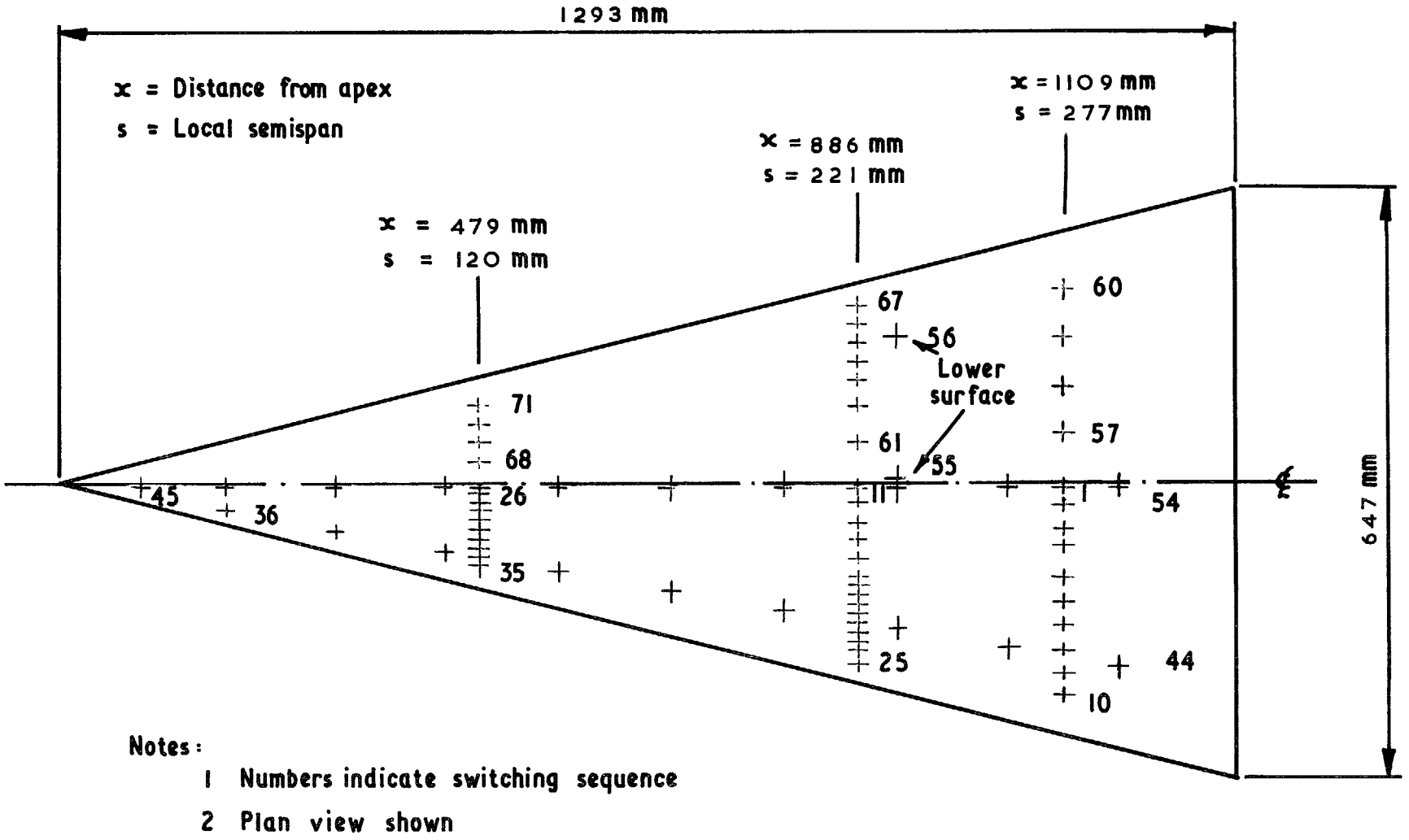

FIG. 5. Locations of heat-flow meters in model.

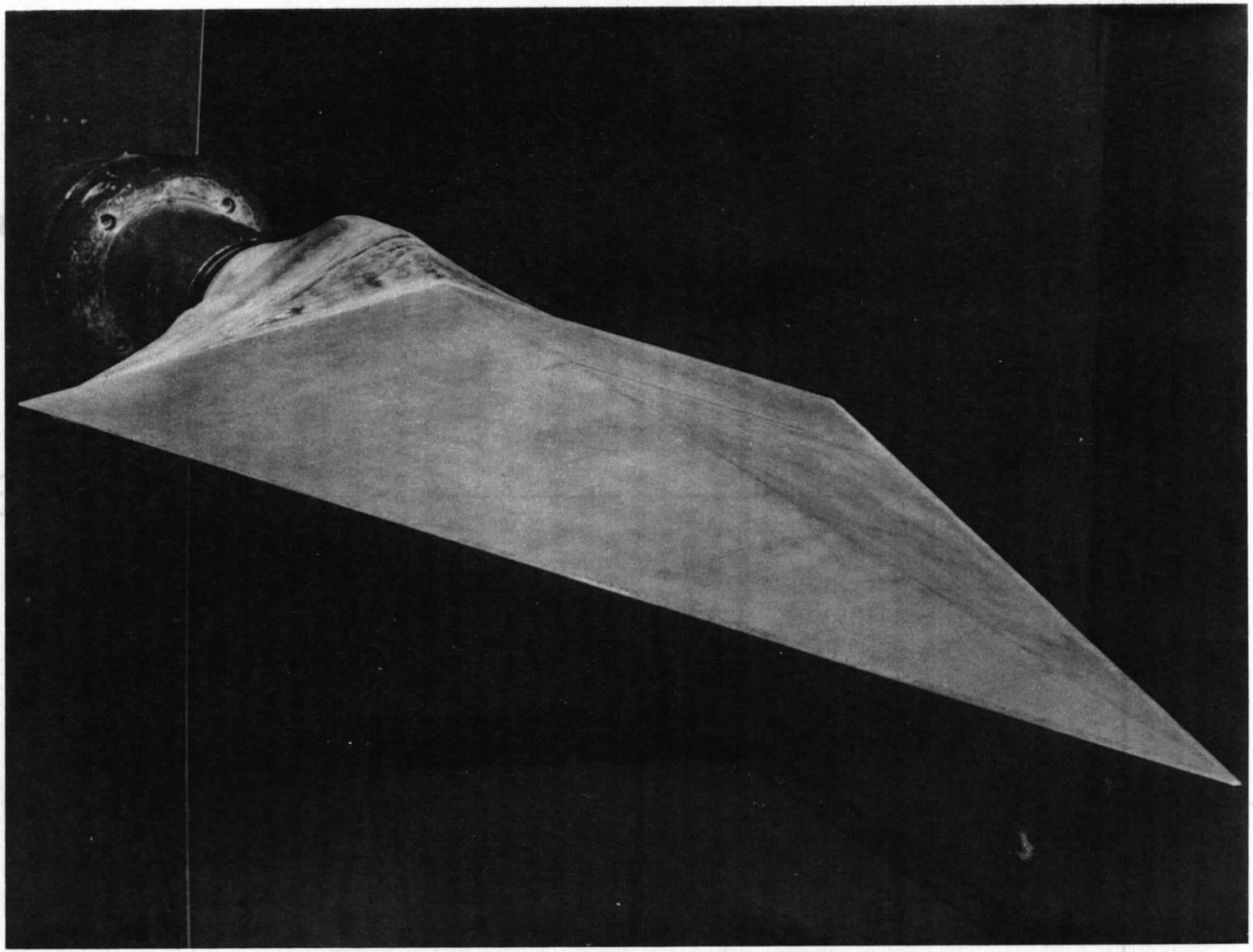

FIG. 6. Model mounted in 8 ft × 8 ft wind tunnel.

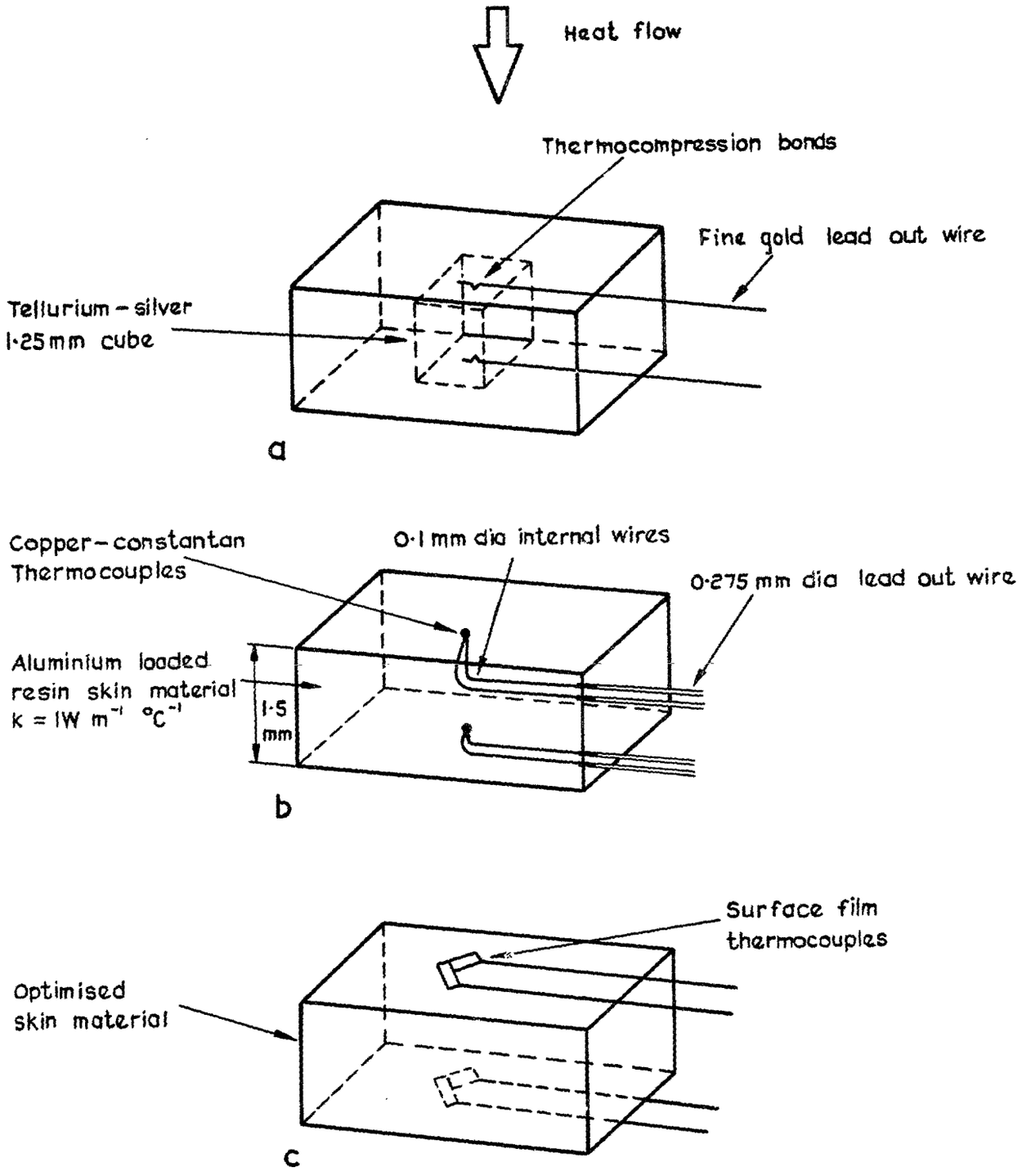

FIG. 7. Types of heat-flow meter.

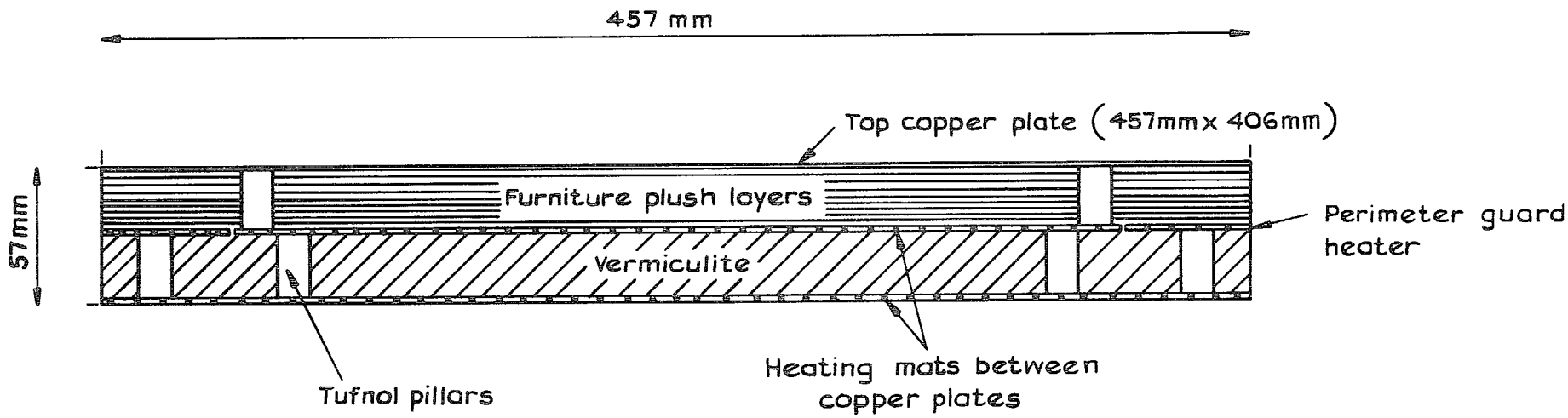

FIG. 8. Section through Hatfield type calibrator for heat-flow meters.

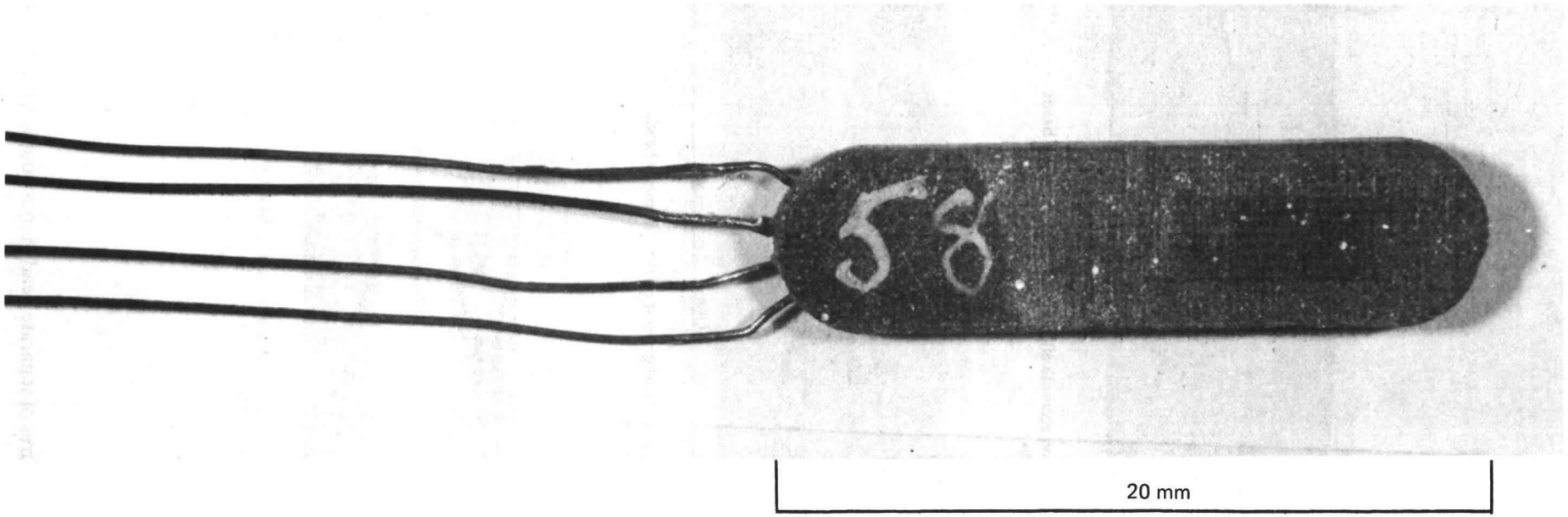

FIG. 9. Separate bead thermocouple heat-flow meter.

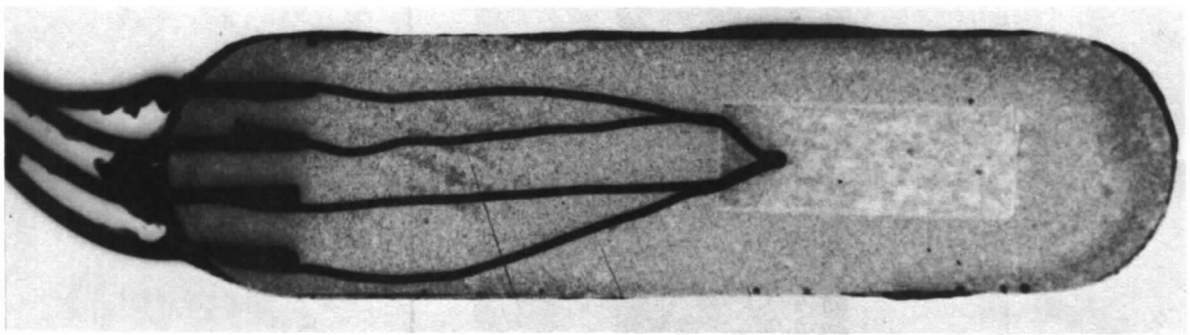

(a) Plan view showing accurate alignment of thermocouple beads in a vertical plane

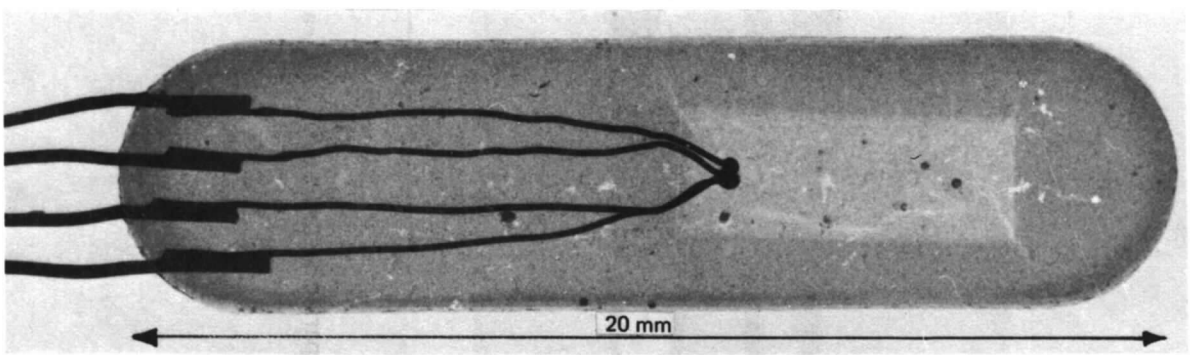

(b) Plan view showing misalignment of thermocouple beads in a vertical plane

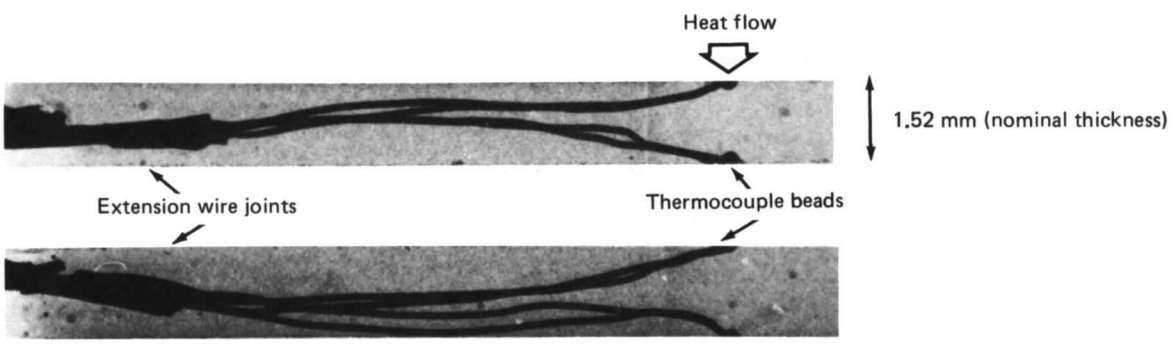

(c) Side view showing position of thermocouple beads and routing of wires for two different meters

FIG. 10. Magnified X-ray pictures of separate bead thermocouple heat-flow meters.

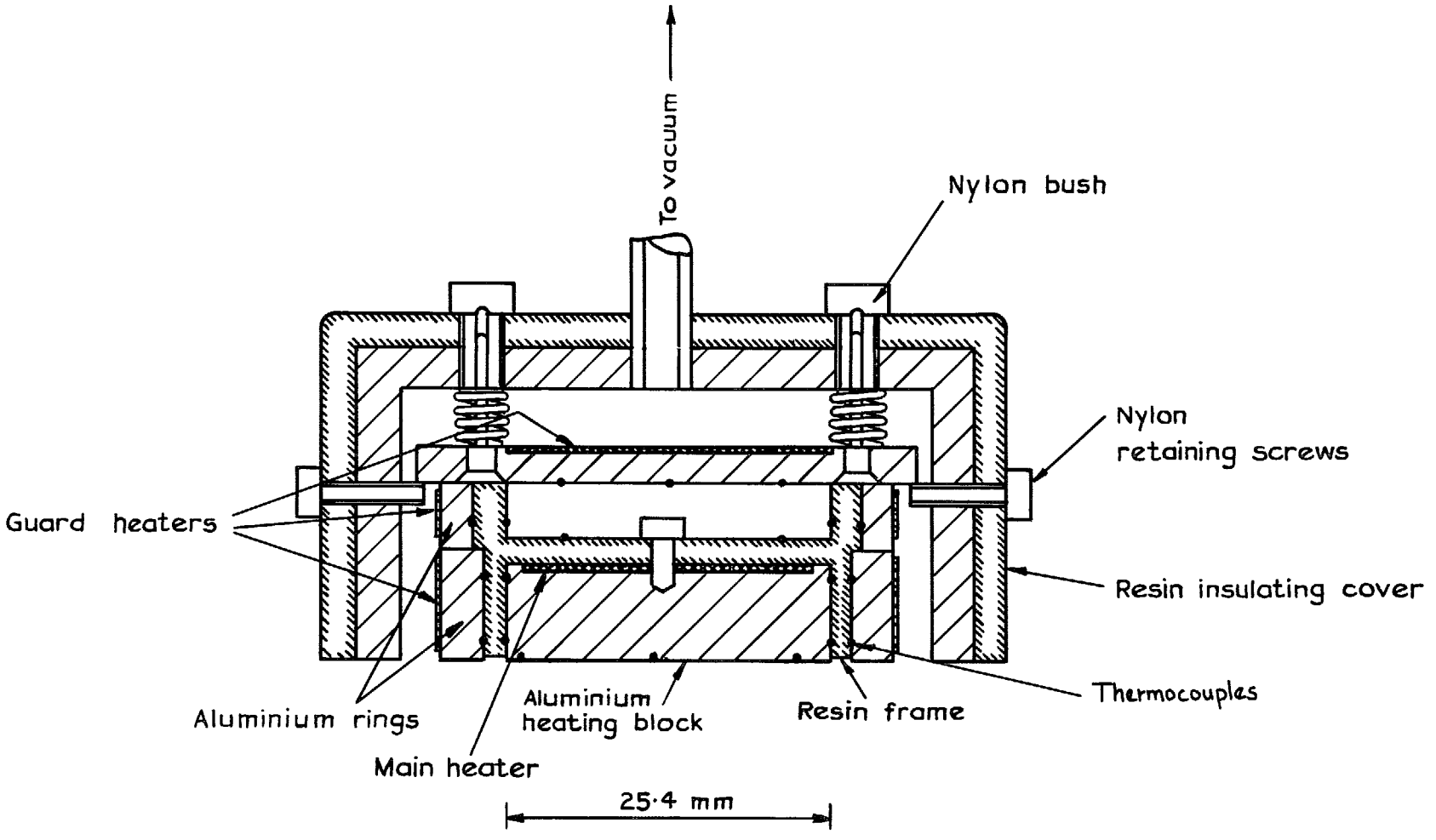

FIG. 11. *In situ* type calibrator.

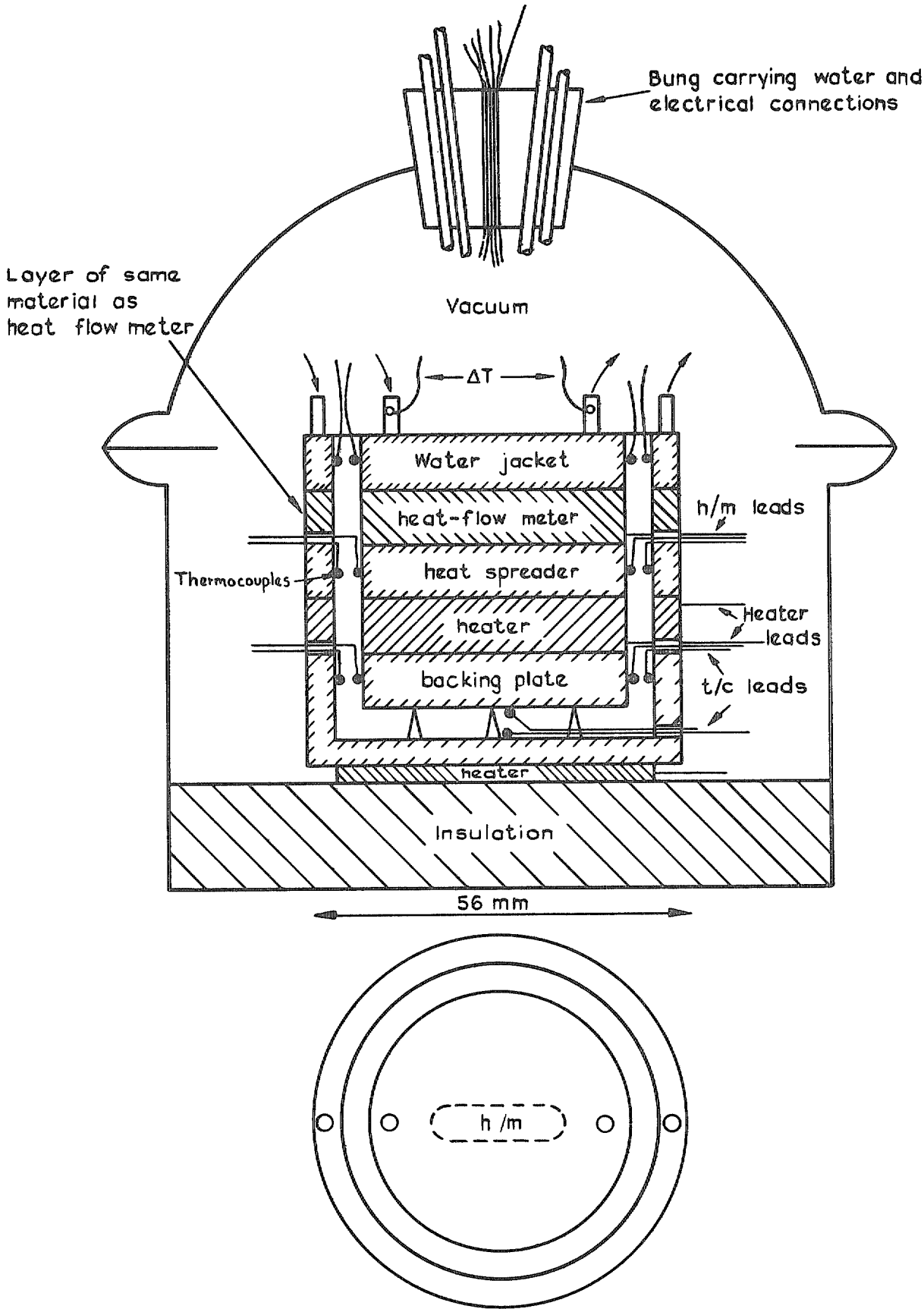

FIG. 12. Modified Lees disc type calibrator.

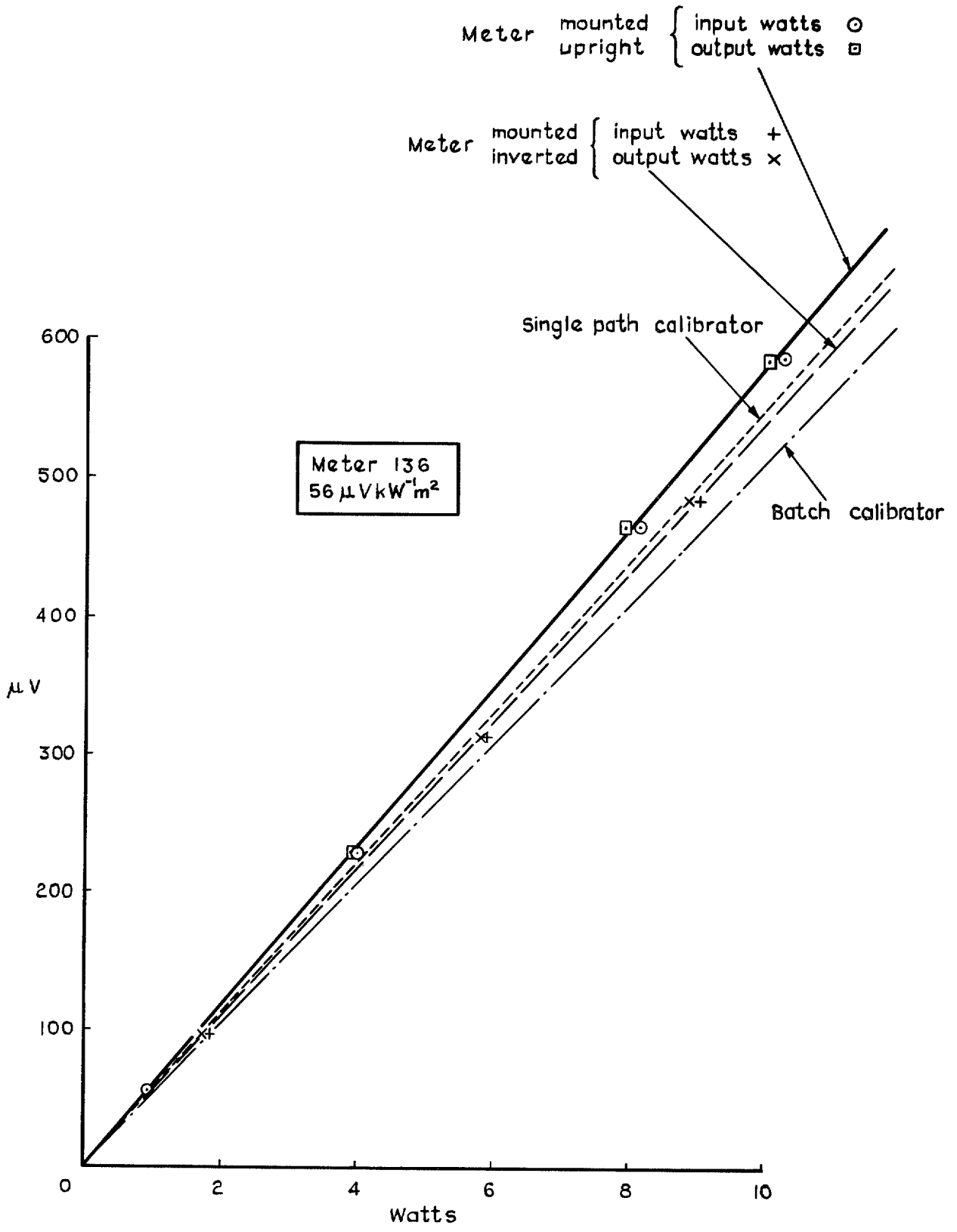

FIG. 13. Heat-flow meter 136—results in modified Lees disc calibrator.

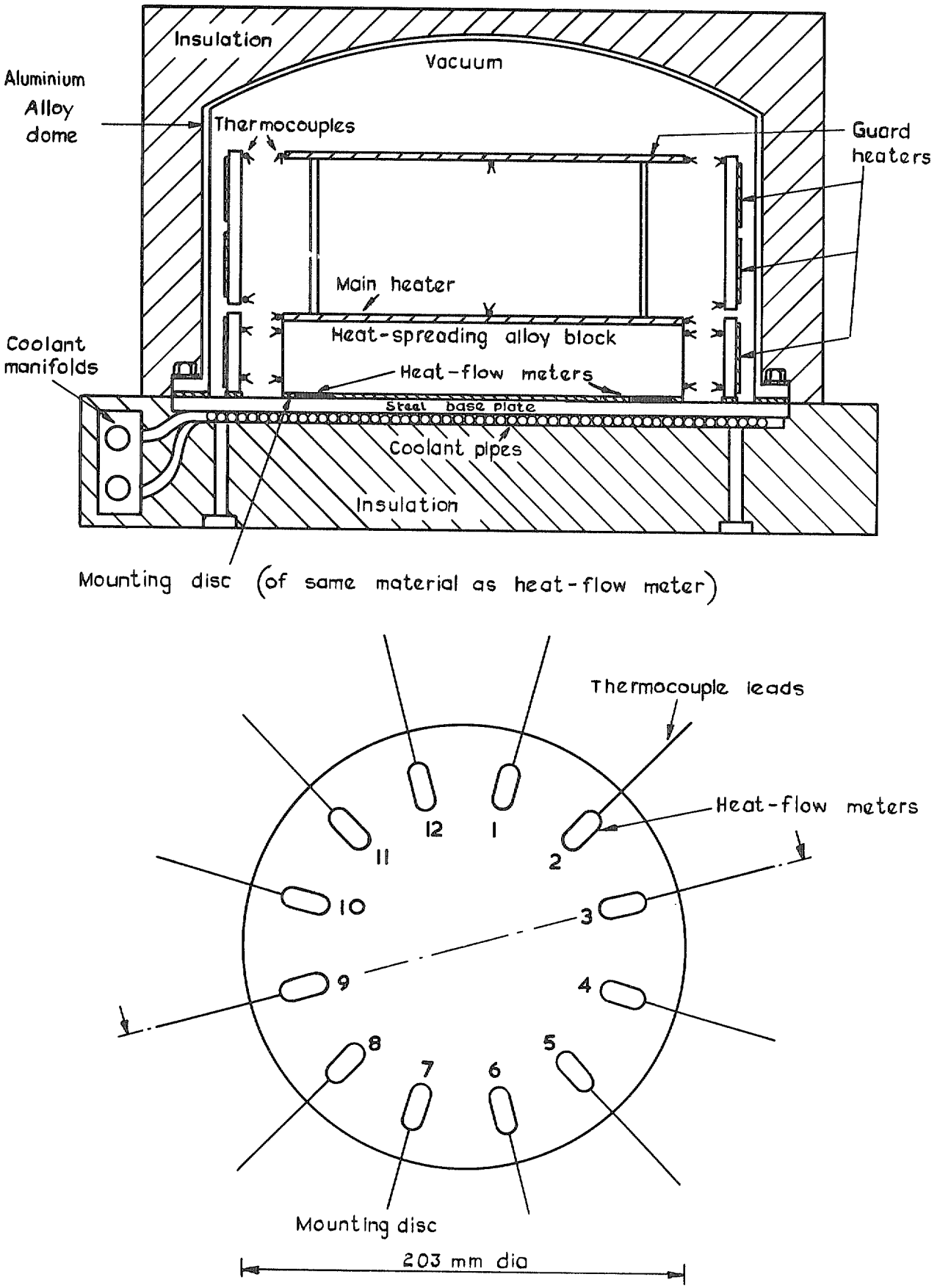

FIG. 14. Batch calibrator.

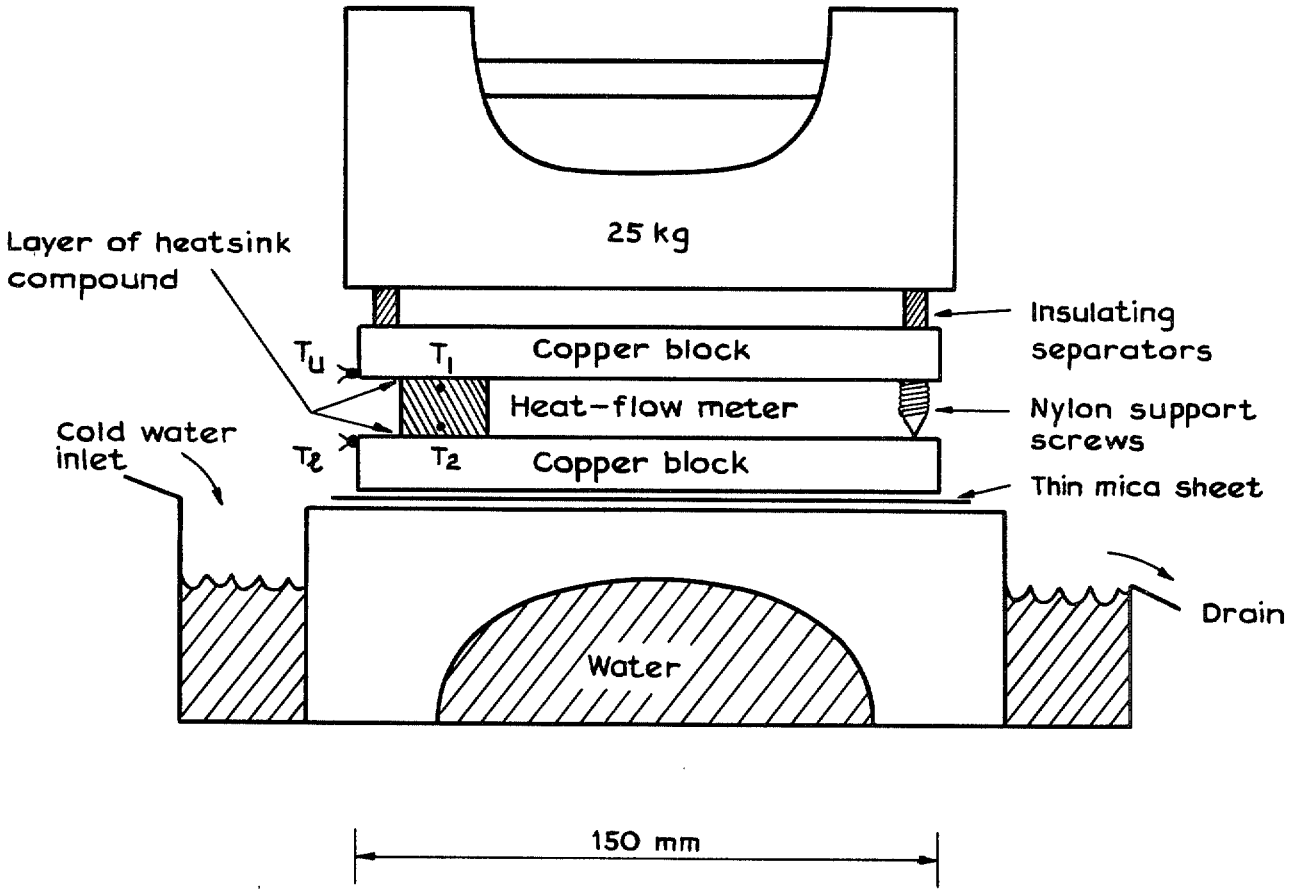

FIG. 15. Copper-block Comparator.

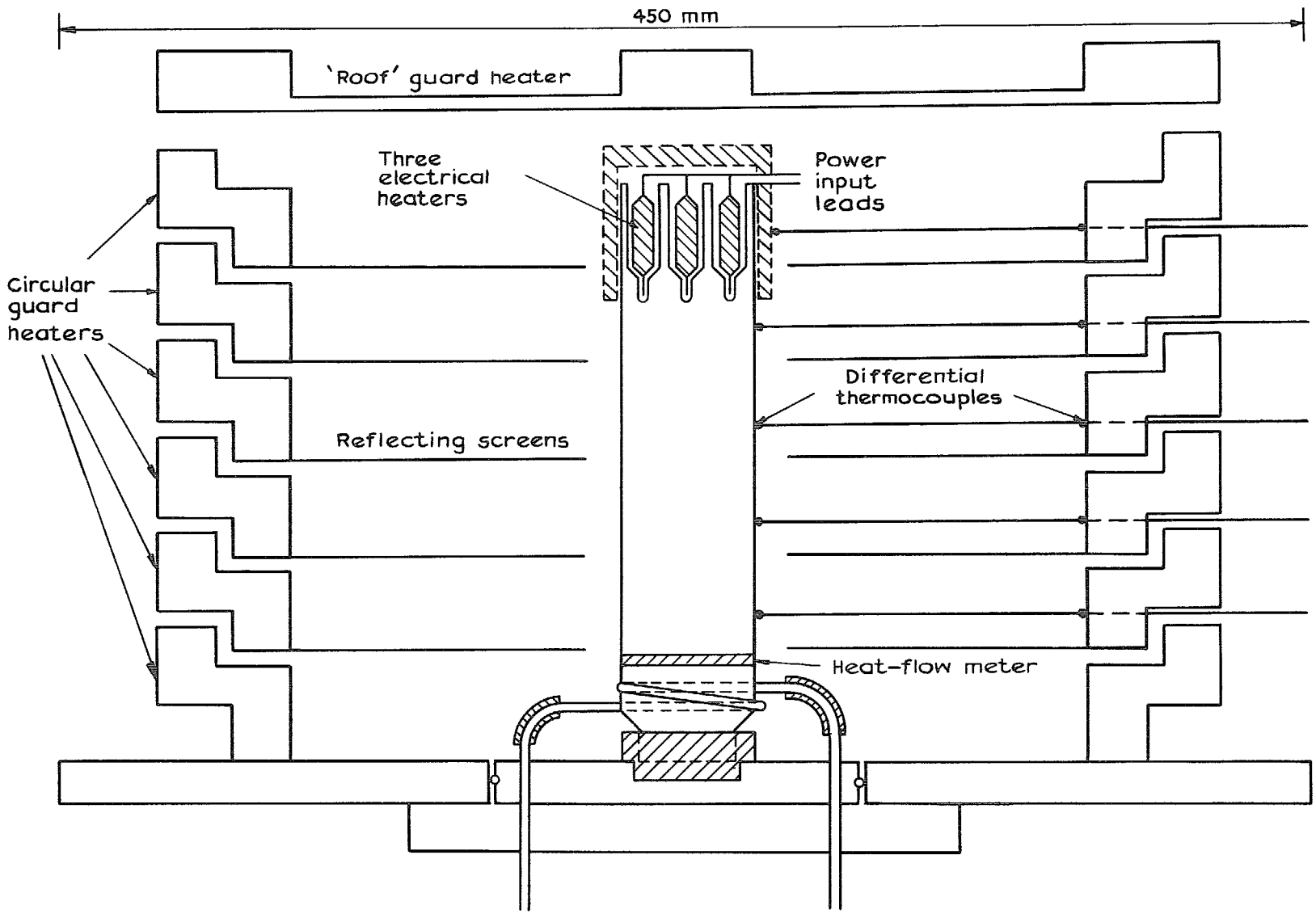

FIG. 16. Single-path conductive calibration system (Asteraki).

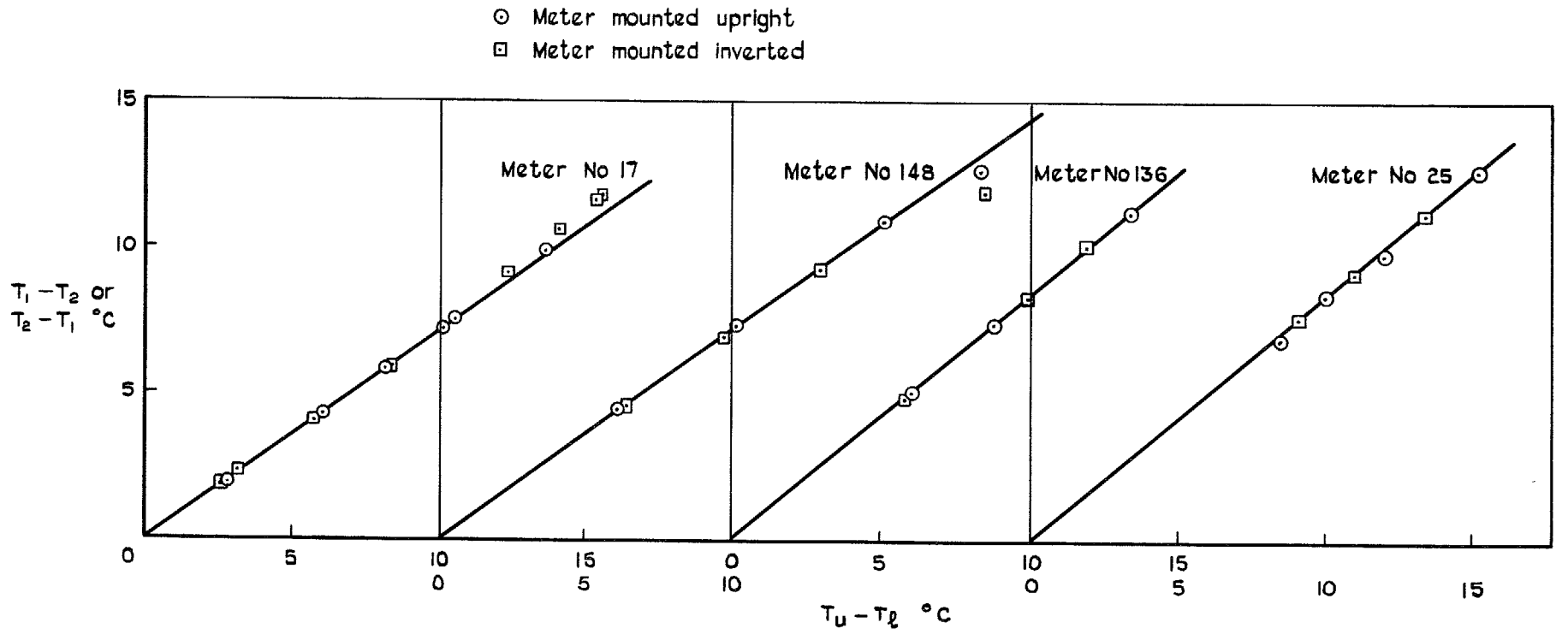

FIG. 17. Typical calibrations in copper-block comparator.

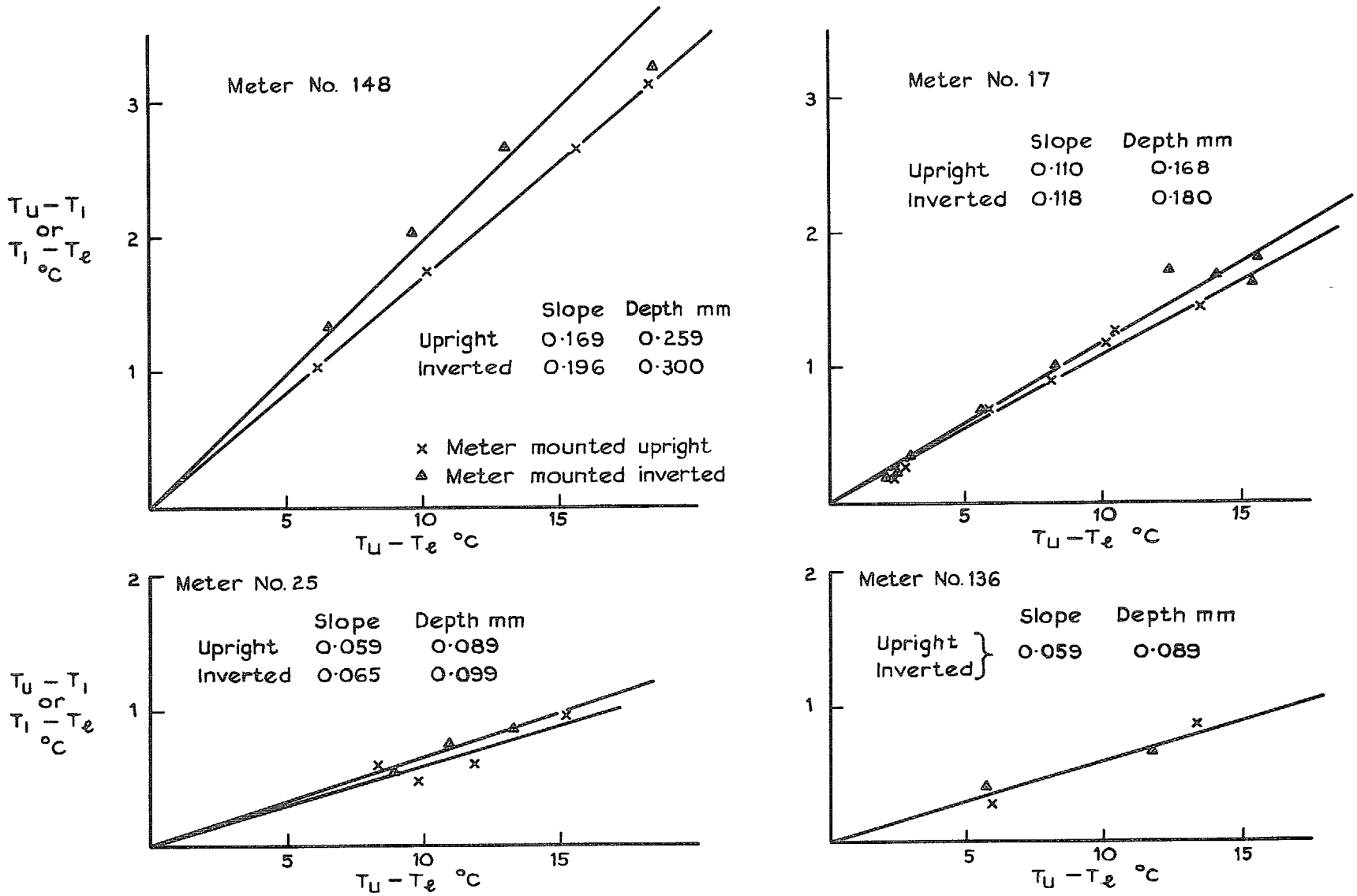

FIG. 18a. Determination of effective depth of surface-temperature thermocouple below surface of heat flow meter.

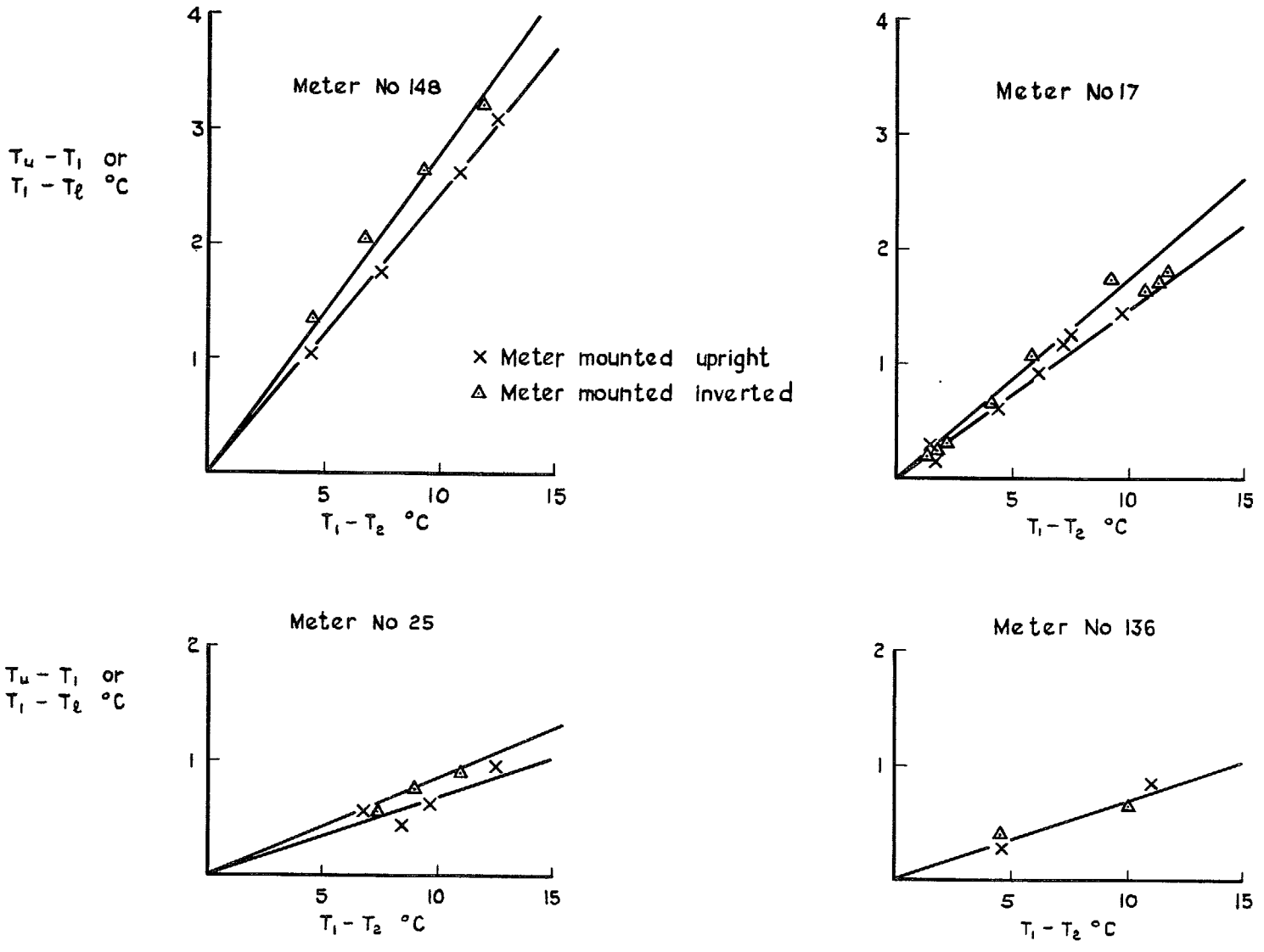

FIG. 18b. Calibration of surface-temperature thermocouple.

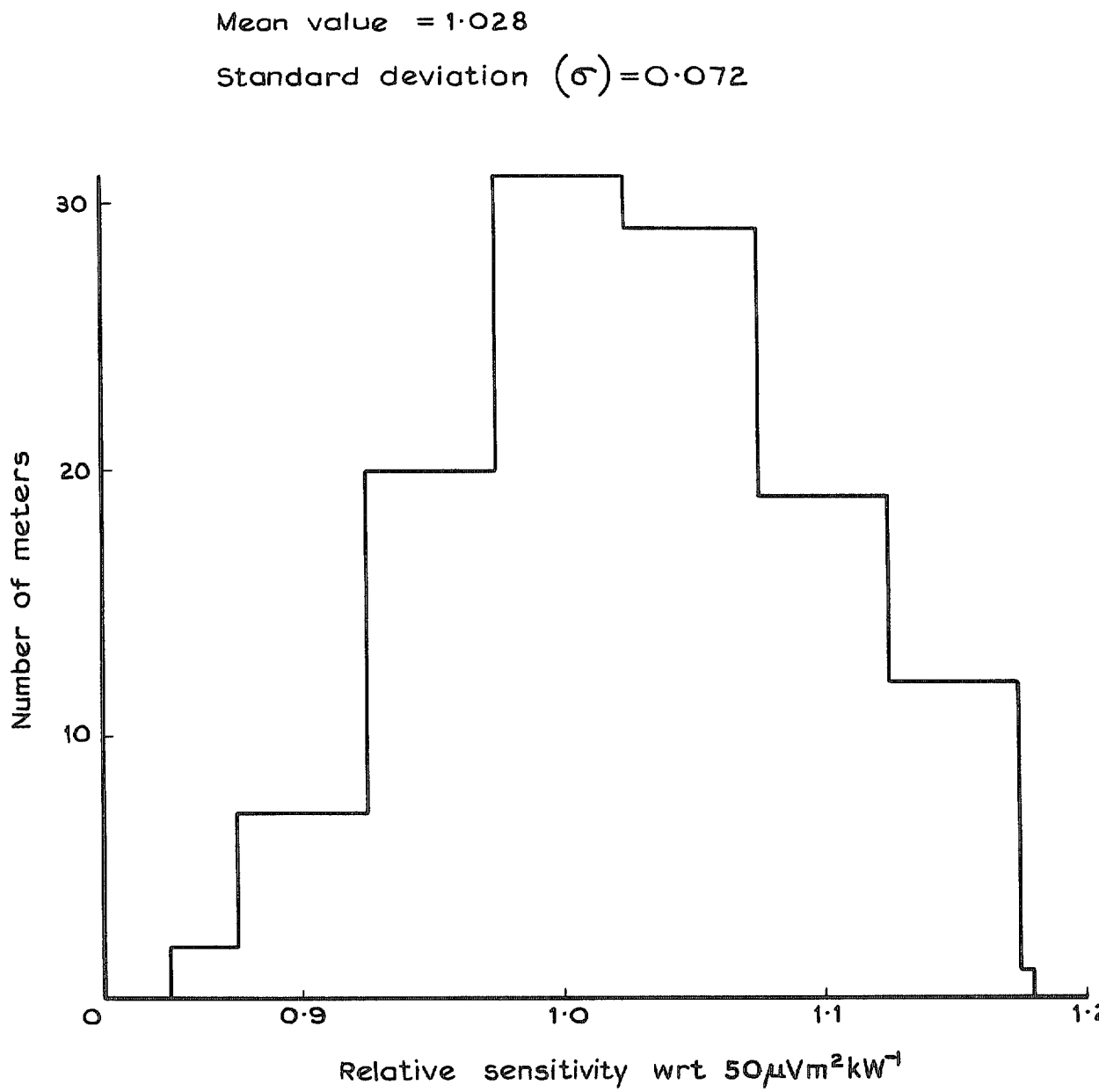

FIG. 19. Histogram of relative sensitivities for 121 separate bead thermocouple heat-flow meters.

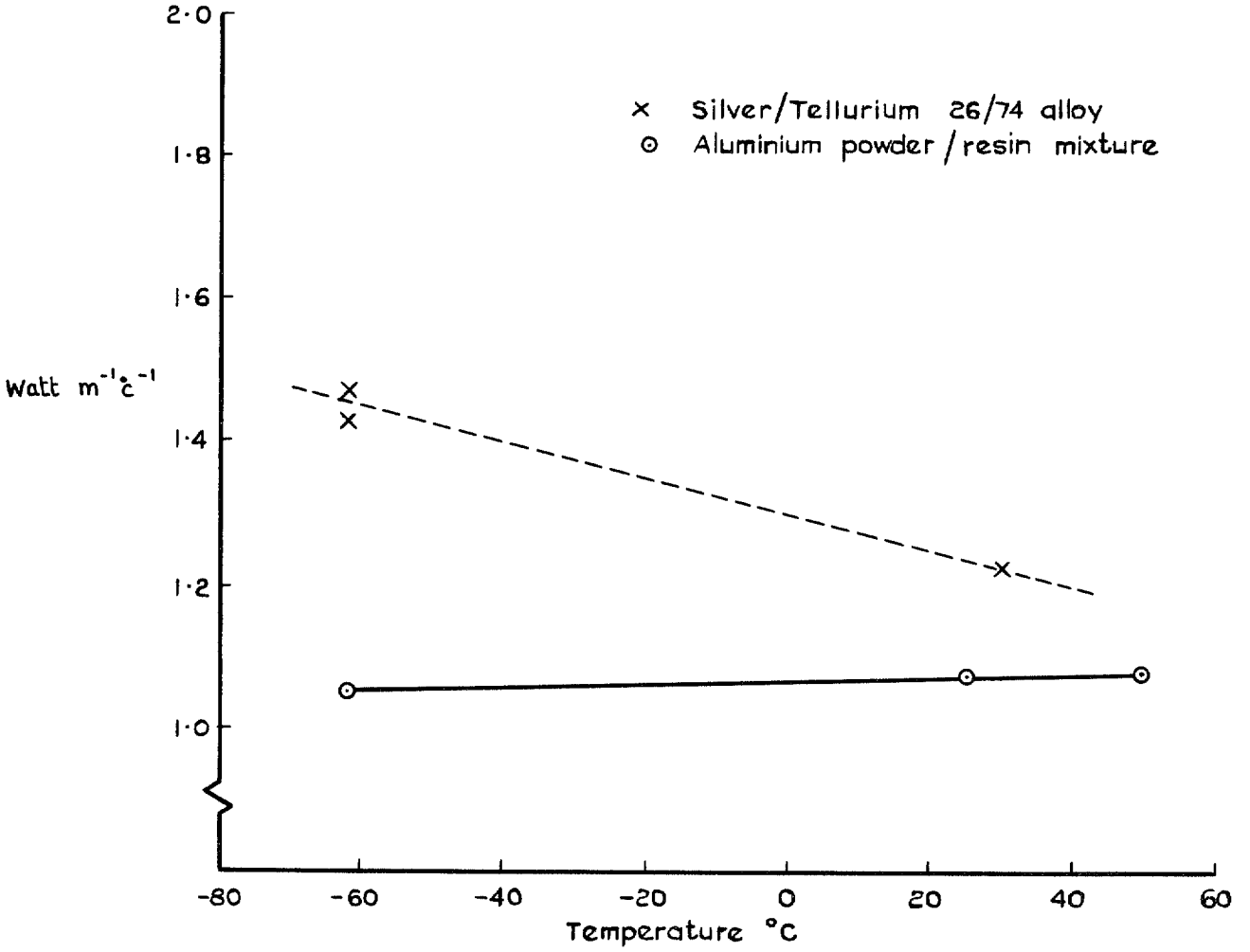

FIG. 20. Thermal conductivity measurements.

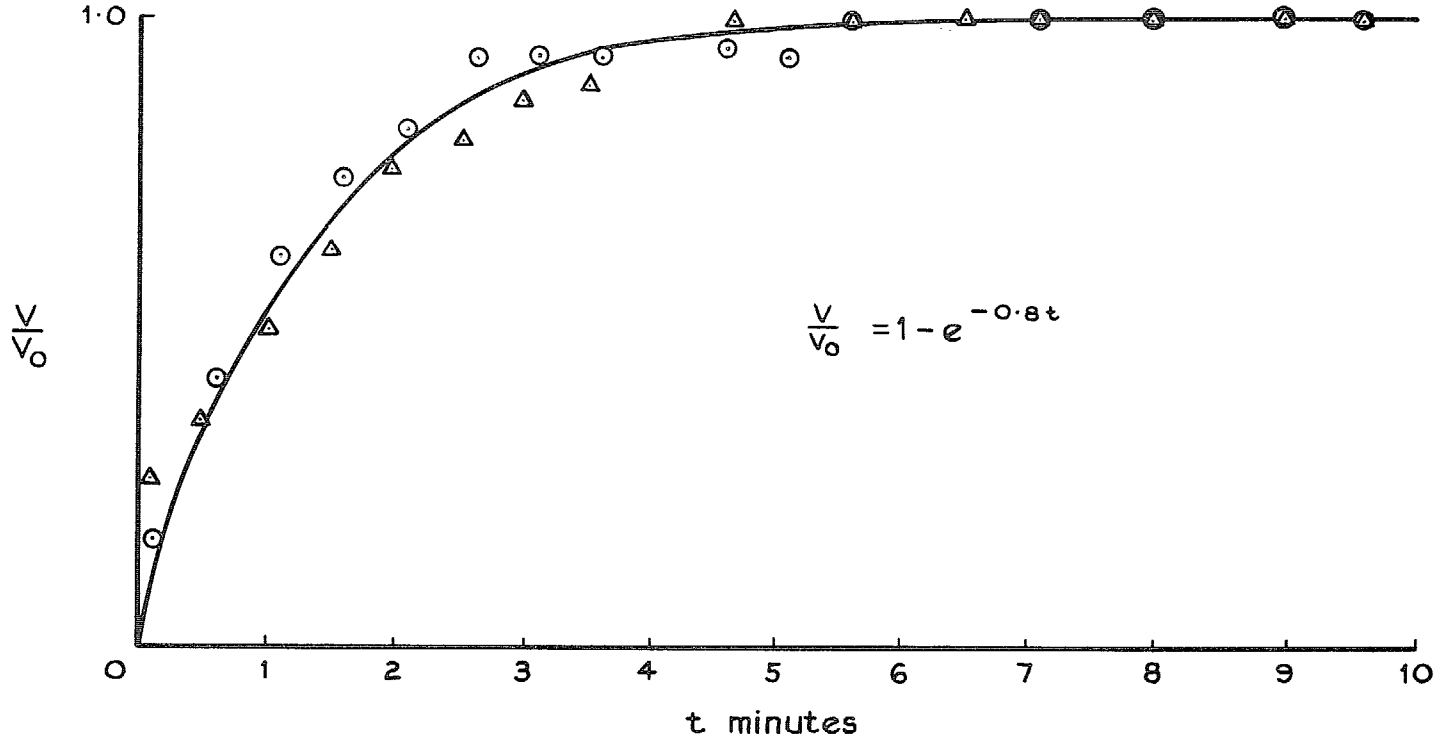

FIG. 21. Response time of heat-flow meter.

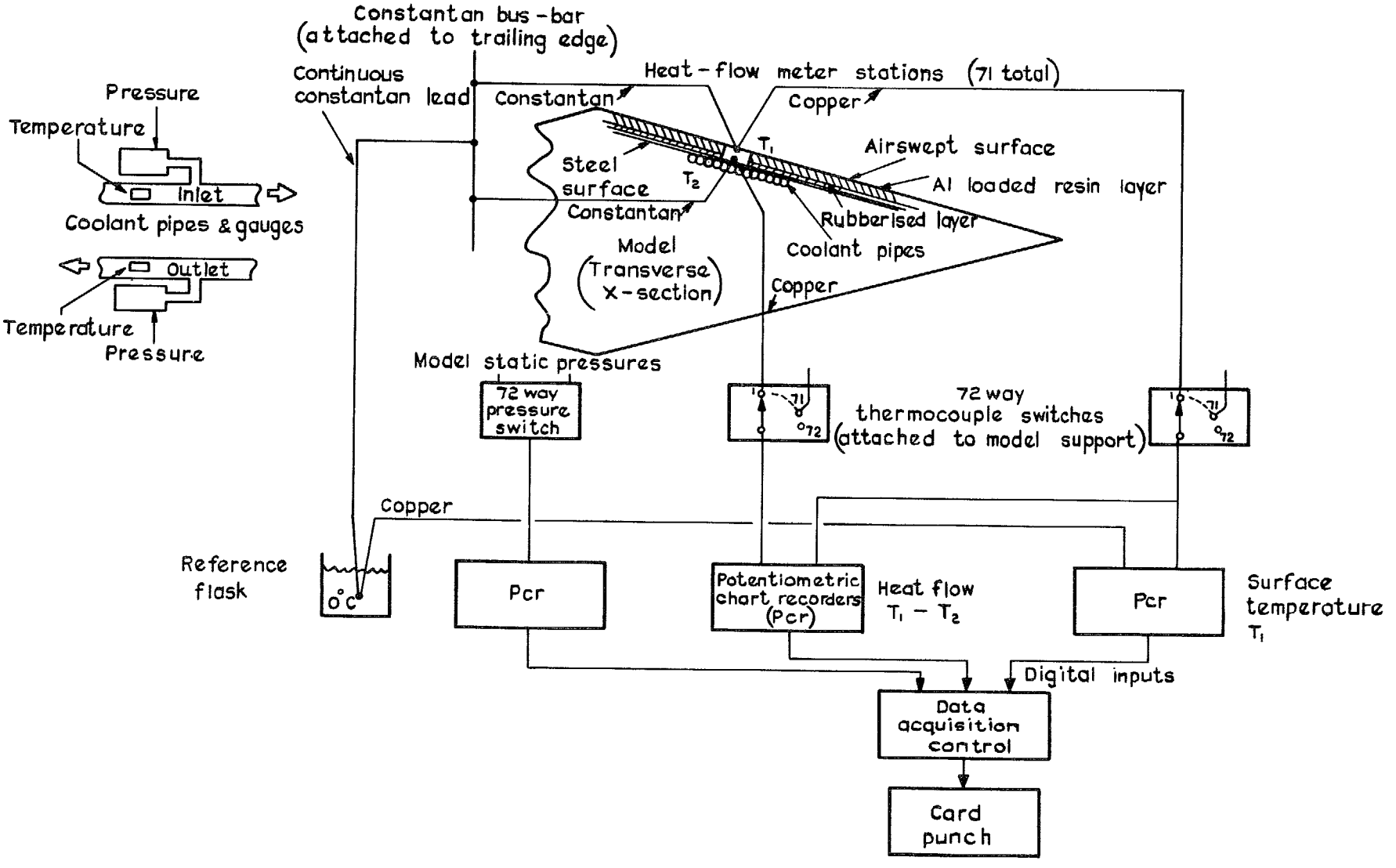

FIG. 22. Schematic heat-flow meter electrical connections.

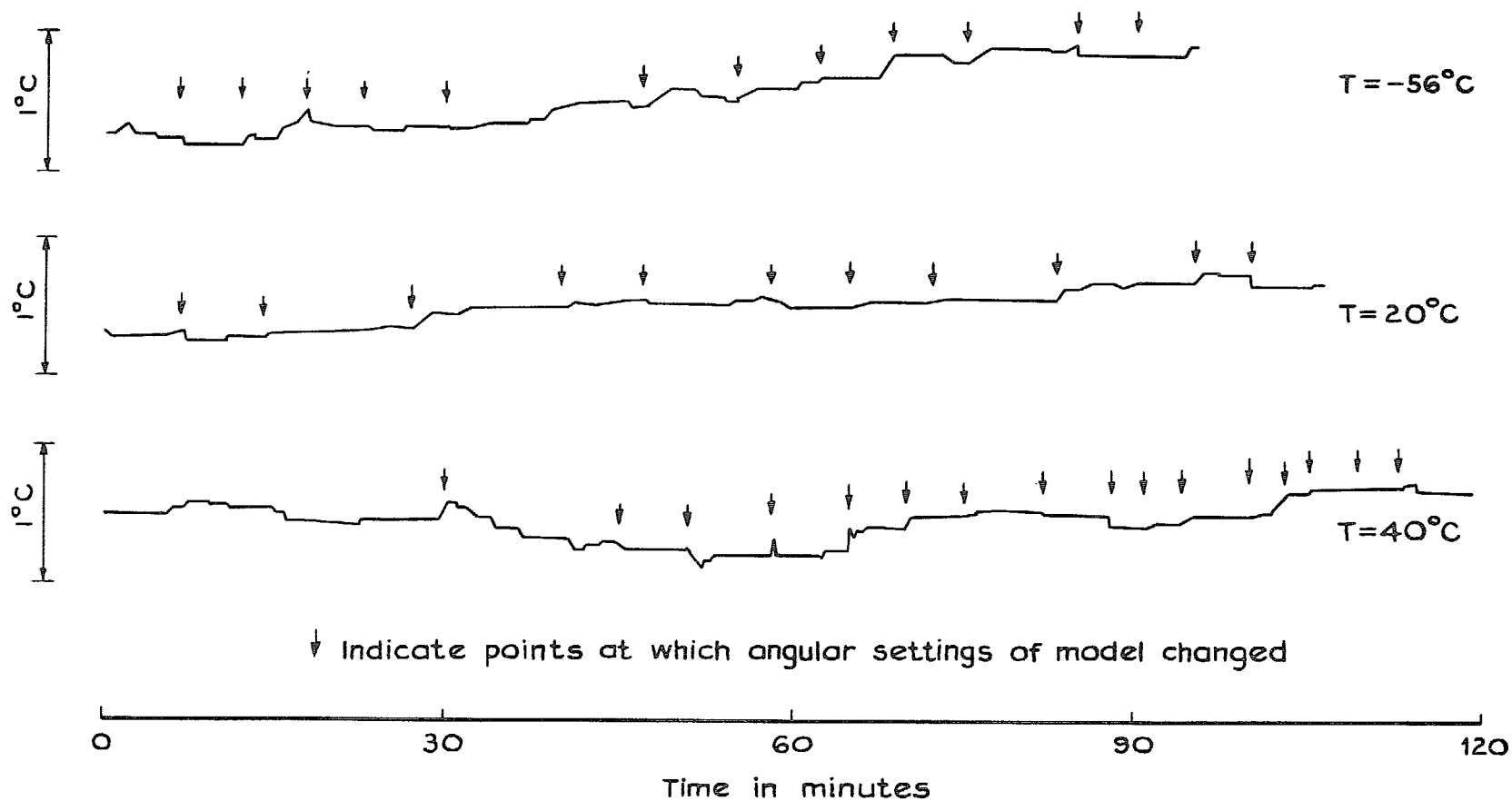

FIG. 23. Examples of variation of model coolant inlet temperature.

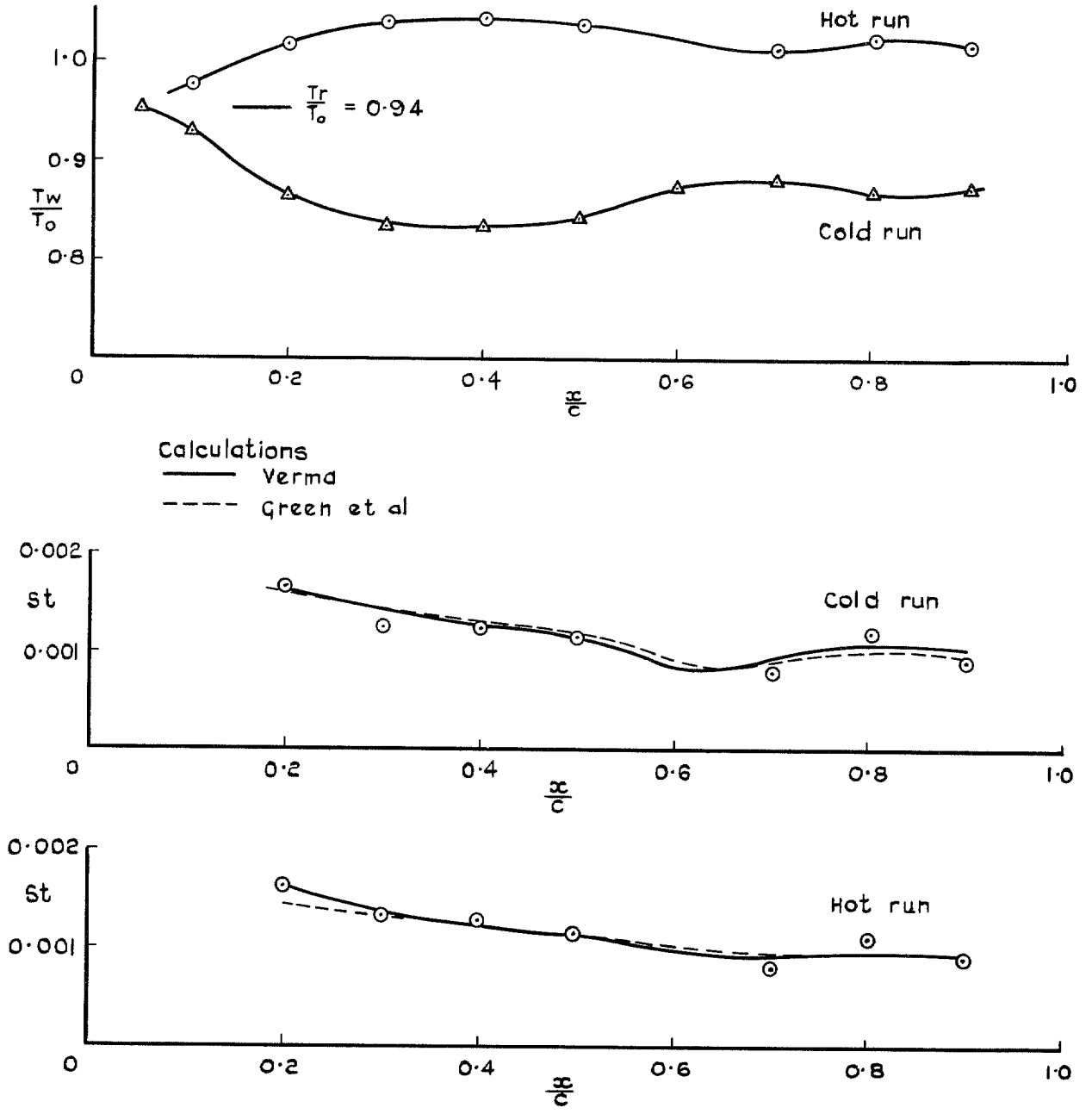

FIG. 24. Surface temperature and Stanton number distribution close to ridge line $M = 2{\cdot}45\ \alpha = 0$.

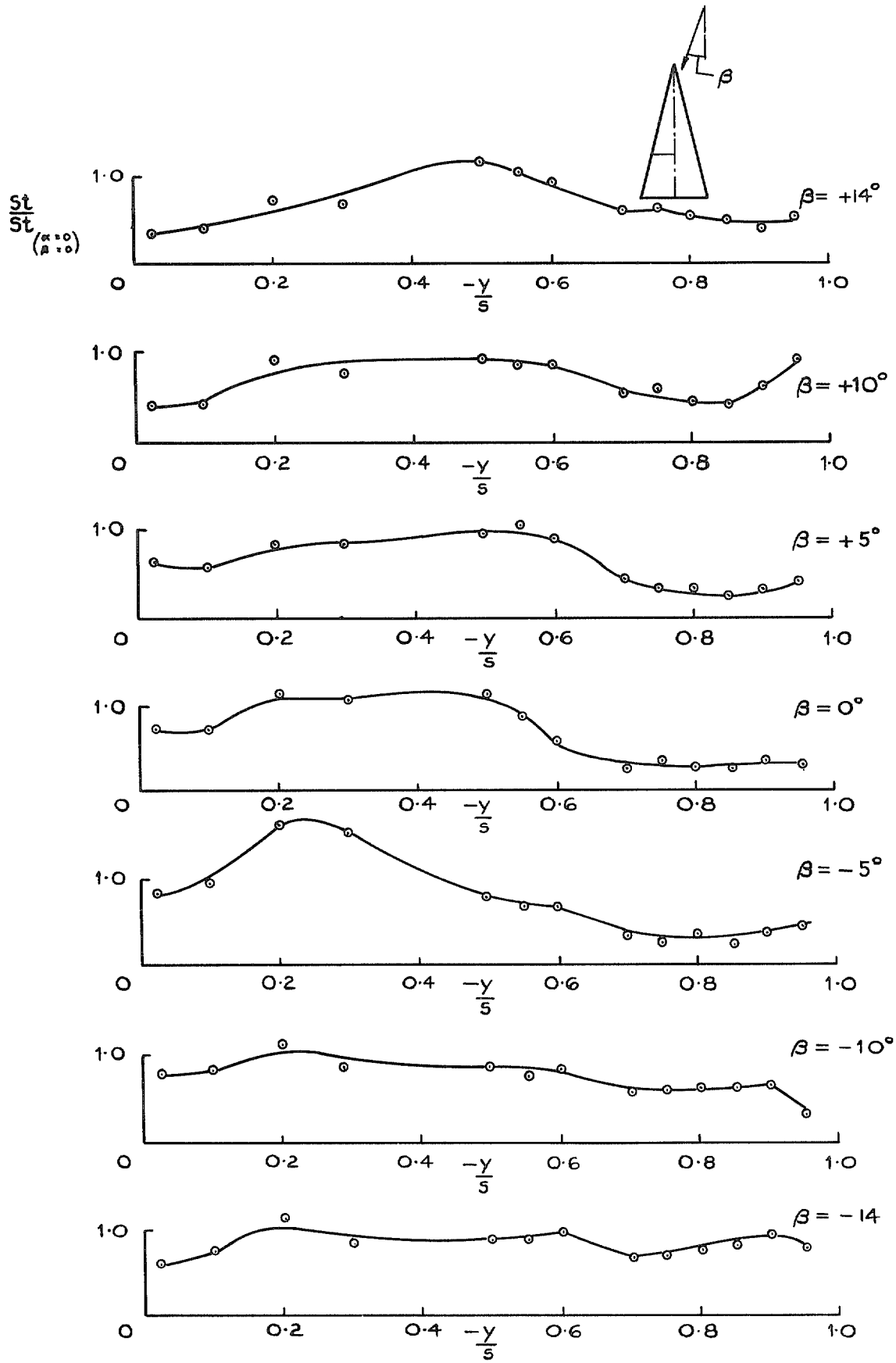

FIG. 25. Variation of St with angle of sideslip $M = 2{\cdot}45$, $\alpha = 10°$.

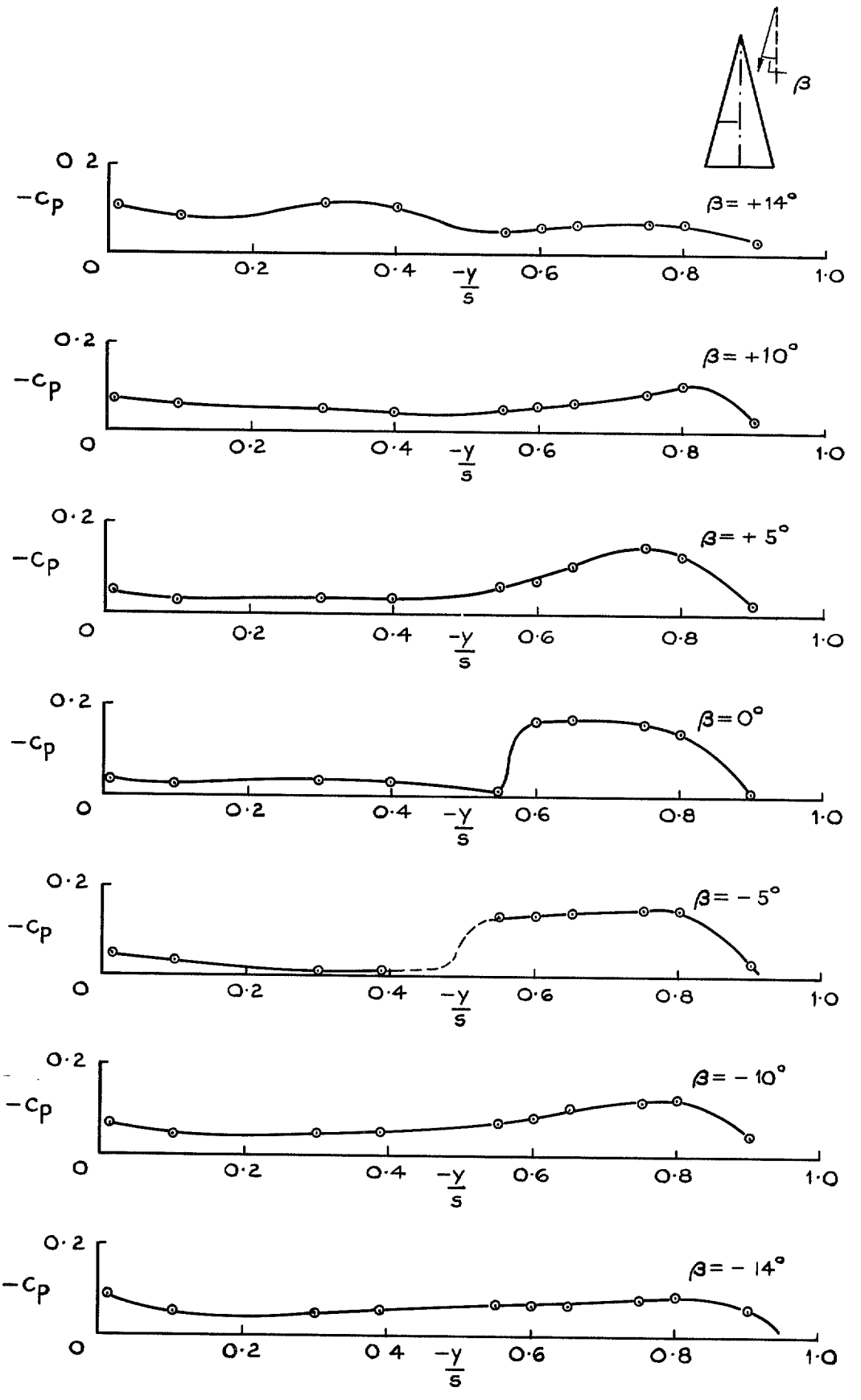

FIG. 26. Variation of pressure coefficient with angle of sideslip $M = 2{\cdot}45, \alpha = 10°$.

Printed in England for Her Majesty's Stationery Office by J. W. Arrowsmith Ltd., Bristol BS3 2NT
Dd. 290278 K.5. 4/77.

HER MAJESTY'S STATIONERY OFFICE

Government Bookshops

49 High Holborn, London WC1V 6HB
13a Castle Street, Edinburgh EH2 3AR
41 The Hayes, Cardiff CF1 1JW
Brazennose Street, Manchester M60 8AS
Southey House, Wine Street, Bristol BS1 2BQ
258 Broad Street, Birmingham B1 2HE
80 Chichester Street, Belfast BT1 4JY

Government publications are also available through booksellers

R. & M. No. 3797

ISBN 0 11 470968 8